BNWL-1441
UC-25

CHARACTERIZATION OF SOME UO_2 AND PuO_2 POWDERS

July 1970

AEC RESEARCH & DEVELOPMENT REPORT

BNWL-1441

BATTELLE NORTHWEST
BATTELLE MEMORIAL INSTITUTE
PACIFIC NORTHWEST LABORATORIES
BATTELLE BOULEVARD, P. O. BOX 999, RICHLAND, WASHINGTON 99352

PACIFIC NORTHWEST LABORATORY
RICHLAND, WASHINGTON
operated by
BATTELLE MEMORIAL INSTITUTE
for the
UNITED STATES ATOMIC ENERGY COMMISSION UNDER CONTRACT AT(45-1)-1830

AEC-RL RICHLAND, WASH.

BNWL-1441

UC-25, Metals, Ceramics,
and Materials

CHARACTERIZATION OF SOME UO_2 AND PuO_2 POWDERS

By

M. J. Barr,(a) M. W. Urie,(a)
J. L. Daniel, and S. J. Mayhan(a)

July, 1970

BATTELLE MEMORIAL INSTITUTE
PACIFIC NORTHWEST LABORATORIES
RICHLAND, WASHINGTON 99352

(a) Now employed by WADCO Corp., a Subsidiary of Westinghouse Electric Corp., under AEC Contract No. AT(45-1)-2170

Printed in the United States of America
Available from
Clearinghouse for Federal Scientific and Technical Information
National Bureau of Standards, U.S. Department of Commerce
Springfield, Virginia 22151
Price: Printed Copy $3.00; Microfiche $0.65

CHARACTERIZATION OF SOME UO_2 AND PuO_2 POWDERS

ABSTRACT

Characterization of nuclear fuel oxide powders typically includes data from chemical analyses (impurities, H_2O, Fl, Cl, etc.) and physical property tests (surface area, particle size and distribution). This paper discusses the physical characteristics of some common UO_2 and PuO_2 powders as determined by B.E.T. surface area, M.S.A. particle size and distribution, and scanning electron micrographs. Powders evaluated include: two commercially produced UO_2 powders, oxalate and nitrate source PuO_2, and burned Pu metal. In addition, oxalate source PuO_2 was calcined at various temperatures to modify the particle properties.

The experimental work discussed herein is believed to be one of the first examples of using a scanning electron microscope to explain the problems associated with physical property measurement of fine powders.

TABLE OF CONTENTS

LIST OF FIGURES

LIST OF TABLES

CHARACTERIZATION OF SOME UO_2 AND PuO_2 POWDERS

INTRODUCTION

Other than composition, the particulate characteristics of a powder are the most important factor influencing its response to densification by compaction and sintering. Conventional powder characterization methods such as particle size distributions, surface area, and impurity analyses all provide useful information; however, these data are generally sensitive to technique and show only relative differences. Fine powders are complex systems and data from a number of characterization techniques is necessary to adequately define the system. Two primary uses of powder characterization data are: (1) for quality control purposes to assure a consistent incoming raw material condition, and (2) as an aid to processing which will influence details of process operations.

The value of characterization data depends on both the accuracy of the measurement and its relevance to the intended processing. At BNW the nuclear oxides (UO_2 and PuO_2) being used in fuel development work are fine powders with an average particle size of 10 microns or less. Problems associated with fine powder characterization include:

1) measurement of one or two characteristics does not adequately classify a powder,
2) identification of the physical property actually being measured,
3) modification of characteristics resulting from measurement technique,
4) segregation resulting from sampling technique.

This paper discusses the characterization of some common UO_2 and PuO_2 powders using conventional techniques and scanning electron micrographs. Variables associated with the equipment and/or the method used are also discussed. The conventional characterization data obtained includes surface area by a modified B.E.T. technique and particle size and distribution using a gravity centrifuge sedimentation technique. Particle morphology is observed by scanning electron microscopy. A general sinterability test was also performed.

SUMMARY

The nuclear oxides currently being used at BNW are fine powders with an average particle size of six microns or less. The average particle size and distribution curves produced show a sensitivity to dispersing technique. Scanning electron micrographs explain this sensitivity and demonstrate apparent limitations in data obtained with particle size and surface area measurements. Problems associated with particle morphology are better defined through use of the scanning electron microscope. Other results of this study indicate that calcination of PuO_2 powders changes the specific surface area but has little effect on particle size distribution. In addition, the normal UO_2 powders analyzed were found to be composed of agglomerates of sub-micron particles or crystallites and accurate particle size analysis was difficult.

PROCEDURE

Test samples are obtained using a modified "thief" technique. The powder to be analyzed is stirred by hand prior to sampling to homogenize the material and minimize the chances of obtaining a nonrepresentative sample. Characterization techniques are discussed below.

A. Particle Size and Distribution

Particle size and distribution are determined by gravity-centrifuge sedimentation using a commercially available M.S.A. (Mine Safety Appliances) particle size analyzer. The powder sample is dispersed in a water-acetone mixture containing a small amount of dispersing agent. The dispersant concentration and degree of agitation are variables which have been investigated and will be discussed in the results section. The particles measured are particles (Stokes equivalent diameter) by definition and the curve produced does not imply a specific state of agglomeration (loosely bound crystallites) or aggregation (firmly bonded crystallites producing fractured surfaces upon separation).

B. Surface Area

Surface area is determined by a modified B.E.T. technique using a commercially available Aminco (SOR-B.E.T.) analyzer. The SOR-B.E.T. technique determined nitrogen adsorption from a nitrogen-helium mixture at a slightly positive pressure. Few technique variables are associated with this measurement (excluding the effects of initial sample heating to 150°C under vacuum to remove adsorbed moisture and gas). Sample preparation variations were not evaluated. Surface area was determined after a number of powder modification operations and the effects of these process operations (prior to mechanical blending of the oxides) on the B.E.T. surface area will be discussed in the results section.

C. Scanning Electron Micro

The scanning electron microscope provides advantages over the conventional electron microscope in that sample preparation does not modify the sample to any significant degree. The image observed is formed with secondary electrons from a scanning beam spot, thus providing excellent depth of field and surface detail.

There are few technique variables to consider with this instrument other than assuring that the sample is representative of the powder lot as a whole. Scanning micrographs supplied valuable particle shape and texture information. The particle morphology data provided a basis for interpreting the results of more conventional characterization techniques.

DISCUSSION OF RESULTS

The powders evaluated included two ammonium-diuranate processed normal UO_2 powders, 93% ^{235}U enriched UO_2, calcined oxalate PuO_2, calcined nitrate PuO_2 and burned Pu metal. The PuO_2 powders were calcined, milled, or otherwise agitated to modify the particulate properties. Characterization data will be discussed in the following order:

A. Normal UO_2
   1. Source A
   2. Source B

B. Enriched UO_2

C. Sinterability of UO_2

D. PuO_2

  1. Calcined Oxalate
  2. Calcined Nitrate
  3. Burned Metal

E. Sinterability of PuO_2

A general comparison of the data obtained will be included in the discussion.

A. Normal UO_2

1. Source A

Source A UO_2 is produced by the ammonium-diuranate precipitate process. The material analyzed was classified by the supplier as "ceramic grade UO_2" with an O/U ratio of 2.15 and a B.E.T. surface area of 9.5 m^2/g.

Analysis at BNW confirmed the O/U ratio and surface area values and also produced the particle size and distribution curves shown in Figures 1 and 2. Figure 1 shows that the average particle size is about 3 microns. Figure 2 was obtained using severe ultrasonic agitation and shows the effects of insufficient dispersant on a size and distribution curve. The up-swing on the 3 drops of

10 g/liter curve is due to compaction in previously settled particle layers. This particular curve points out a source of bias in particle size obtained using centrifugal sedimentation. The earliest layers formed from gravity and low rpm sedimentation will compress slightly when higher centrifugal forces are applied. This compaction contributes to experimental error. The 5 and 10 drops of 10 g/liter would indicate that dispersant concentration is not critical above the minimum (in this case >3 but <5 drops of 10 g/liter solution).

A scanning electron micrograph of as-received Source A UO_2 (Figure 3) shows the material to consist of large agglomerates of very small particles or crystallites. These agglomerates appear to average about two to five microns in diameter. This agrees with particle size data in Figure 1.

A quantity of Source A UO_2 was examined in the SEM after wet ball milling for four hours. The effect of milling on the agglomerate size and distribution is readily apparent from comparing micrographs of the wet milled UO_2 (Figure 4) with the as-received (Figure 3). The surface area after milling was 9.3 m^2/g indicating that milling had no effect on this property. The surface area appears to be influenced more by the morphology of individual particles or crystallites than by the state of agglomeration. A higher magnification micrograph (approximately 20,000 X) still fails to define the nature of Source A UO_2 crystallites (see Figure 5).

2. Source B

The Source B UO_2 analyzed was also produced by the ammonium-diuranate precipitate process. Analysis for O/M ratio and B.E.T. surface area indicated values of 2.15 and 3.5 m^2/g, respectively. The particle size distribution curve (Figure 6) for this material indicates an average particle size of about two to three microns.

A scanning electron micrograph (Figure 7) shows that the material consists of agglomerates of fine particles or crystallites. The basic similarity in appearance between the Source B and Source A powders (compare Figure 7 with Figure 3) is believed a result of similar production methods. The variation in surface area and particle size is believed a result of small variations in precipitation and oxidation-reduction conditions.

B. Enriched UO_2

The enriched UO_2 analyzed contained 93.16% ^{235}U. Enriched UO_2 was produced through conversion of uranium hexafluoride. Analysis shows the O/U ratio and surface area to be 2.08 and about 2.0, respectively. The particle size and distribution curve shown in Figure 8 indicates an average particle size around two to three microns. The center portion of the curve in Figure 8 (dotted line) is theorized as data points could not be determined due to lack of definable layers. Reasons for this effect are still being investigated.

A 2,000X micrograph of enriched UO_2 (Figure 9) would indicate that the powder consists of loose agglomerates of from 1 to 10 microns in diameter. The 20,000X micrograph (Figure 10) of an agglomerated area shows that agglomerates consist of many well-shaped crystallites varying from 0.1 to 1 micron in diameter. The uniform dispersion of loose agglomerates (Figure 9) and relatively smooth crystallite surfaces (Figure 10) would indicate a less active powder than the Source A or Source B materials.

C. Sinterability of UO_2

Test groups containing six to ten pellets each were pressed and sintered to determine the relative sinterability of each powder. Table 1 below contains fabrication data, sintering conditions, and sinterability results.

TABLE 1

FABRICATION AND SINTERING CONDITIONS USED FOR UO_2 SINTERABILITY TESTS

	Source A	Source B	Enriched
Powder Condition	As-Received	As-Received	As-Received
Binder[1]	None	None	1/8% PVA-1% Butyl-Stearate
Pressing Pressure	30,000	20,000 - 40,000	20,000 - 40,000
Green Density (g/cc)	5.17	5.42 and 5.96	5.69 and 6.17
Sintering Temp. (°C)	1,675	1690°C	1,675
Sintering Time (hours)	2	6	4
Sintering Atmosphere	Argon-8% H_2	Argon-8% H_2	Argon-8% H_2
Sintered Density (g/cc)	10.49	10.32 and 10.51	10.09 and 10.24
% Theoretical[2]	95.62	94.07 and 95.81	93.06 and 94.48

NOTES: 1. Enriched UO_2 would not press well without a binder-lubricant. A small amount of lubricant (Butyl-Stearate) was also applied to the die and punch for pressing of Source A and B powders.

2. Theoretical density was calculated on the basis of 10.97 grams/cc for normal UO_2 and 10.84 grams/cc for 93.16% enriched UO_2.

The sintered densities would indicate that all three UO_2 powders sinter reasonably well. The 2% TD difference between the enriched UO_2 and the

Source A and B may be partially attributed to the difference in particle morphology (Figures 3, 7, and 10).

D. PuO_2

1. Calcined Plutonium Oxalate

The surface area and volatile content of PuO_2 powder obtained from calcined oxalate precipitate varies with the calcine temperature. As-received powder is precalcined by the supplier at 500 ± 50°C. To lower the volatile content, improve the stability with respect to moisture sorption, and reduce the carbon content (oxalate residue), the as-received oxalate source PuO_2 is usually recalcined to about 700°C. Test samples were also recalcined to 1000°C. Surface area, particle size distributions, and scanning electron micrographs have been obtained on as-received (450°C calcine), 700°C and 1000°C recalcined oxalate source PuO_2.

The B.E.T. surface area of oxalate source PuO_2 calcined to 450, 700, and 1000°C was 38, 9.2, and 1.4 m^2/g, respectively. Particle size distribution curves (Figure 11) show that calcine temperature has little effect on the size distribution. This was verified with scanning micrographs (Figures 12 and 13) of 450°C and 1000°C calcined powder. Figures 12 and 13 show essentially no change in crystallite or agglomerate shape and form.

The typical oxalate source PuO_2 agglomerate is composed of angular platelets generally arranged into a "rosette" structure about a nucleation center or point. The agglomerates are formed during precipitation of plutonium oxalate $[Pu(C_2O_4)_2 \cdot 6H_2O]$ and vary in size from approximately 1 micron to about 30 microns (see Figure 14). The average size is around 6 microns. Calcination to 450°C produces $PuO_{2.0}$ powder containing 2 to 3 percent volatiles (primarily oxalate residue and moisture). Calcination to 450°C also changes the crystallite surfaces from a "fuzzy" or rounded structure to a sharper angular platelet (compare Figure 14 with Figure 15). Calcination at temperatures above 450°C has little observable affect on surface texture or particle size, however, the decrease in surface area from about 40 m^2/g to 1.4 m^2/g infers that presintering or aggregation occurs - evidently in the more closely packed agglomerate center.

Evidence of sintering (aggregation or bonding of agglomerates) during calcining to 1000°C was observed when recalcined powders were ultrasonically agitated for various lengths of time. Figures 16 and 17 contain scanning micrographs of powders having no agitation, 15 minute ultrasonic agitation, and 120 minute ultrasonic agitation. Figure 16 shows that the plutonia agglomerates were broken into platelets and smaller agglomerates (or aggregates) after 15 minutes. After 120 minutes very few agglomerates remained intact and the powder consisted mainly of individual crystallites. Agglomerate subdivision after 15 minutes is probably the reason for the slight shift of the 450°C curve in Figure 11 from the 700 and 1000°C curves. Figure 17 shows that after 120 minutes of agitation many aggregated particles still exist with the majority of crystallites existing as extremely fine submicron particles. The remaining aggregates are believed to be the center portion of larger aggregates.

The transition of calcined oxalate source PuO_2 "particles" from a loose agglomerate to a more firmly bonded aggregate structure as calcine temperature increases is clarified by data from particle size analysis obtained on 700 and 1000°C calcined material. Size distribution curves obtained after 15 minutes and after two hour agitation of 1000°C calcined material (Figure 18) show a definite shift with increased agitation. The series of curves obtained after agitation of 700°C calcined powder (Figure 19) also shows a shift. The long "tail" on the maximum time curves in both Figure 18 and 19 is indicative of a relatively high percentage of submicron particles. The series of curves in Figure 19 is interesting as the gradual break-up of mildly aggregated material is shown as a function of agitation time. Scanning micrographs of this material are not shown; however, they confirm the extent of aggregate breakup.

Experiments to determine the effect of dispersant concentration on particle size produced effects similar to that obtained with Source A UO_2 (compare Figure 20 with Figure 2). Inadequate dispersant permits excessive agglomeration, faster settling, and some compaction at higher rpm's.

2. Calcined Plutonium Nitrate

Plutonia (PuO_2) may be obtained from plutonium nitrate solution by evaporation and calcination. As with calcined plutonium oxalate, the particulate properties and impurity levels are related to the calcine temperature. The material evaluated was precalcined by the supplier to about 450°C. The surface area for plutonium nitrate calcined to 450°C, 650°C, 800°C and 1000°C was 6.3, 5.7, 3.5 and less than 1 m^2/gram, respectively. Particle size and distribution curves for powder calcined at the aforementioned temperatures are shown in Figure 21. Calcination temperature does not appear to significantly influence the size distribution curve. The small variations between curves in Figure 21 are believed due to minor variations in measuring technique.

Scanning electron micrographs (Figure 22) show the calcined nitrate source PuO_2 particles to be spheroids ranging from submicron to about 5 microns in diameter. Agglomerates are frequent which may account for the relatively large number of "particles" above 5 microns in Figure 21. No information was obtained on the relative strength or state of aggregation within the agglomerates.

3. Burned Pu Metal

A third source of PuO_2 is through controlled burning (oxidation) of Pu metal slabs. Particle size and surface area are influenced by the initial burning temperature. Temperatures of from 600°C to 1000°C have proved adequate. Material from 600°C oxidation appears finer and more uniform in appearance. The surface area of the experimental batch used for analysis was 7.0 m^2/gram after burning in wet helium at 950°C and was 10.7 m^2/gram after 72 hour ball milling using Al_2O_3 media. Particle size distribution (Figure 23) as well as scanning electon micrographs (Figure 24) were obtained on ball milled material. The average particle size appears to be between 1 and 2 microns. The slope of the curve denotes an asymmetric distribution with an excessive number of submicron particles.

Scanning electron micrographs show the powder to be composed of spheroids and oblong particles in relatively loose agglomerates. The average particle size appears less than one micron. Figure 24 also shows occasional hexagonal or angular particles 5 to 10 microns long. There appears to be good agreement between the particle size data obtained by gravity-centrifuge and the observed particle size (scanning micrographs).

Table II

SINTERABILITY OF VARIOUS SOURCE PuO_2 POWDERS

PuO2 Source	Surface Area m^2/g	Green Density[1] at 30,000 psi	Pellet Ejection Pressure-psi	Sintered Density % TD (11.46 g/cc)	Density Range	Dia. (Max-Min)
Oxalate						
625°C Calcine	17.4	56.30	14,000	92.30	91.0 - 94.3	0.005 in.
Burned Pu Metal 72 hour Ball Mill	10.7	66.2	5,500	97.00	96.5 - 97.5	0.002 in.
Nitrate						
450°C Calcine	6.3	55.9	15,500	92.38	91.7 - 92.8	0.0045 in.
650°C Calcine	5.7	59.7	6,100	91.73	90.7 - 93.0	0.003 in.
800°C Calcine	3.5	62.2	5,000	91.54	90.5 - 92.1	0.0035 in.
1000°C Calcine	<1.0	63.0	3,300	91.17	90.4 - 91.8	0.003 in.

Note 1 Green density is based on 11.46 gms/cm^3 theoretical

E. Sinterability of PuO_2

Test pellets of calcined plutonium nitrate, burned plutonium metal, and calcined plutonium oxalate (recalcined at 625°C) were sintered in wet helium at 1550°C for two hours. The helium was bubbled through water prior to entering the sintering furnace.

Table 2 shows the relative sinterability of PuO_2 from the three sources currently being considered for fast reactor fuel. Of the three source powders, calcined oxalate PuO_2 was the most difficult to press as a single oxide. Pressing difficulty was evidenced by pellet diameter variation, pellet ejection pressure, and the increased dwell time required. Each average in Table 2 represents an eleven to fourteen pellet average.

The sharp angular platelets of oxalate source PuO_2 are considered as contributing to pressing difficulty as agglomerates of these platelets would grip the die surface and inhibit pressure distribution within the pellet. The high pellet ejection pressure (14,000 psi) and 0.005 inch hourglassing in the sintered pellet support this assumption.

Recalcination of calcined nitrate PuO_2 had a small but consistent effect on sintered pellet density. The decrease from 93.38 to 91.17 percent theoretical density is uniform with higher recalcine temperature producing slightly lower sintered densities.

The high green and sintered density of burned Pu metal is largely the result of the finer particle size of that material. The particle size of burned Pu metal after ball milling was about 1 micron (see Figure 23) whereas the particle size of both oxalate and nitrate source PuO_2 was about 6 microns (see Figures 11 and 21).

CONCLUSIONS

To understand the nature of fine powders, it appears necessary to use data obtained from a number of characterization techniques. To obtain maximum benefit from the data obtained, it is also necessary to understand the relative value and/or any limitations associated with that data. The following conclusions that may be drawn from this study are:

1) The scanning electron microscope has proven to be a valuable characterization tool for providing morphological perspective on fine powders as well as clarifying data produced by conventional techniques.
2) Calcination of PuO_2 powders is effective in changing surface area, but does not appear to modify the particle size distribution, or visual (scanning micrograph) surface to a significant degree. The change in surface area is believed due to the healing of microcracks and probable presintering of the particle core.
3) The normal UO_2 powders analyzed were too fine to be accurately analyzed using the M.S.A. particle size analyzer. Scanning electron micrographs of normal UO_2 powders show them to be agglomerates of submicron or ultra-fine crystallites.
4) Ultrasonic agitation and subsequent particle size analysis may be a useful technique in demonstrating the relative strength of agglomerates or aggregates and in determining the temperature at which the sintering phenomena commences.

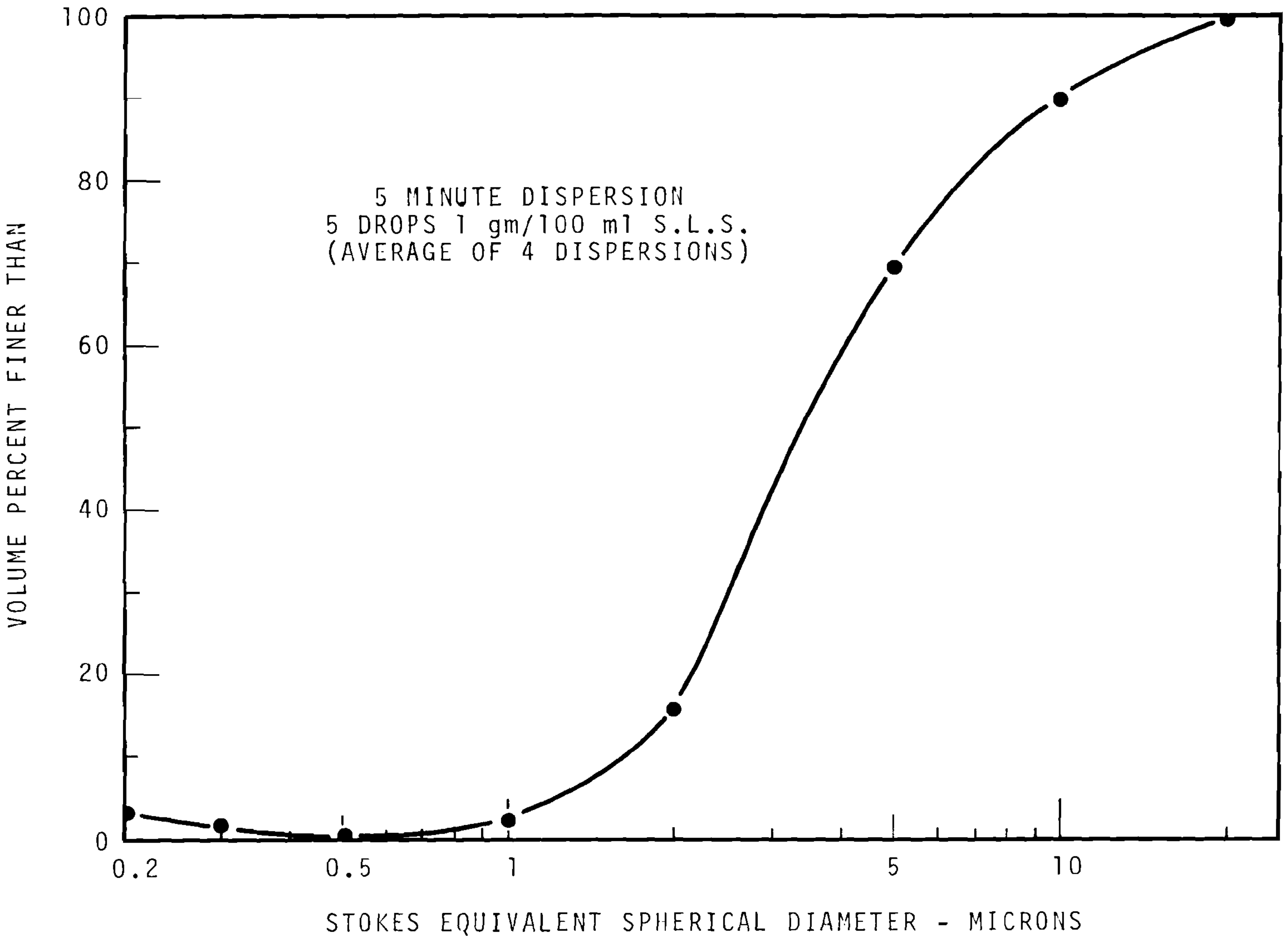

FIGURE 1. PARTICLE SIZE OF AS-RECEIVED SOURCE A UO_2

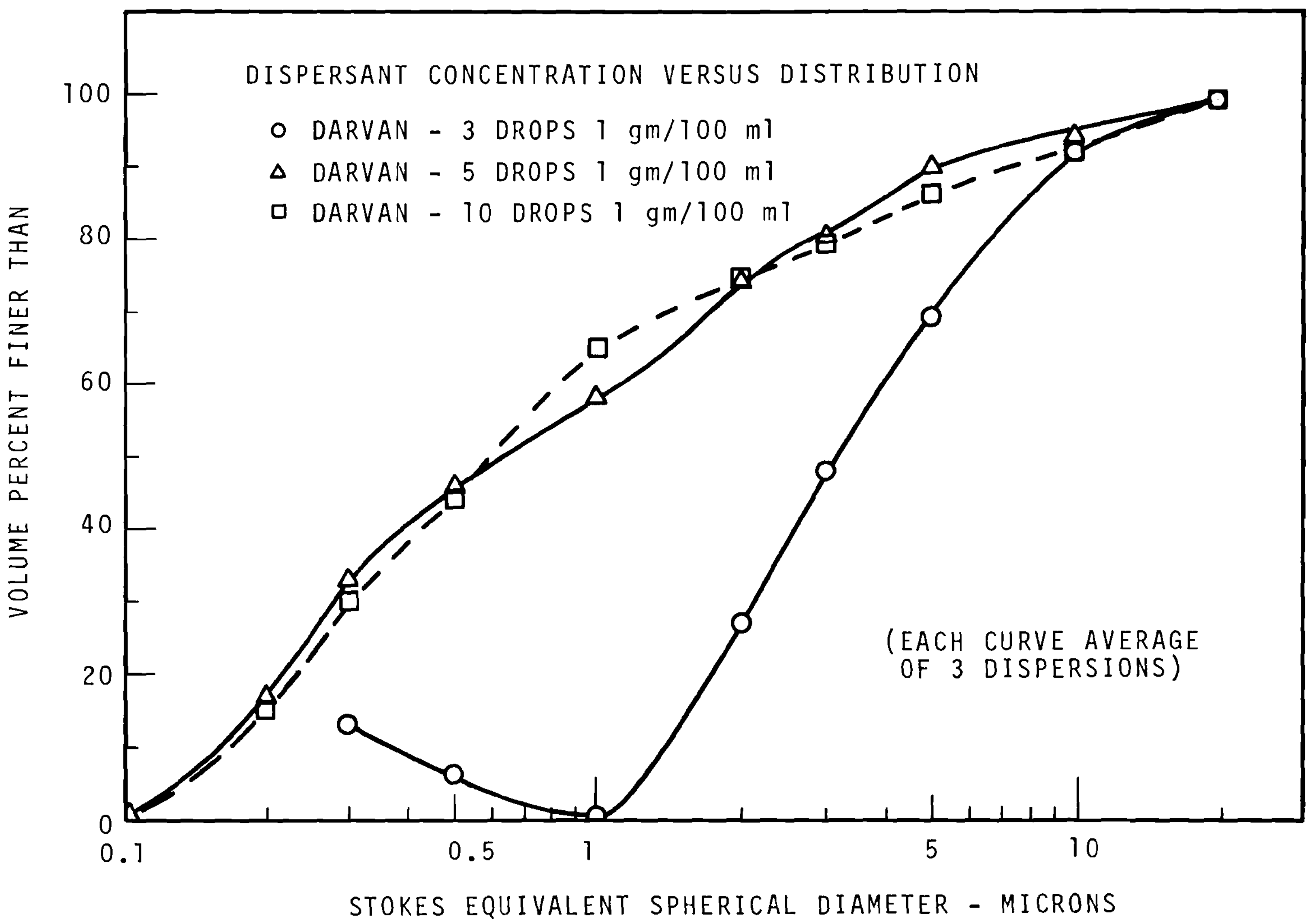

FIGURE 2. EFFECT OF DISPERSANT CONCENTRATION ON PARTICLE SIZE OF AS-RECEIVED SOURCE A UO_2 (2 HOUR DISPERSION)

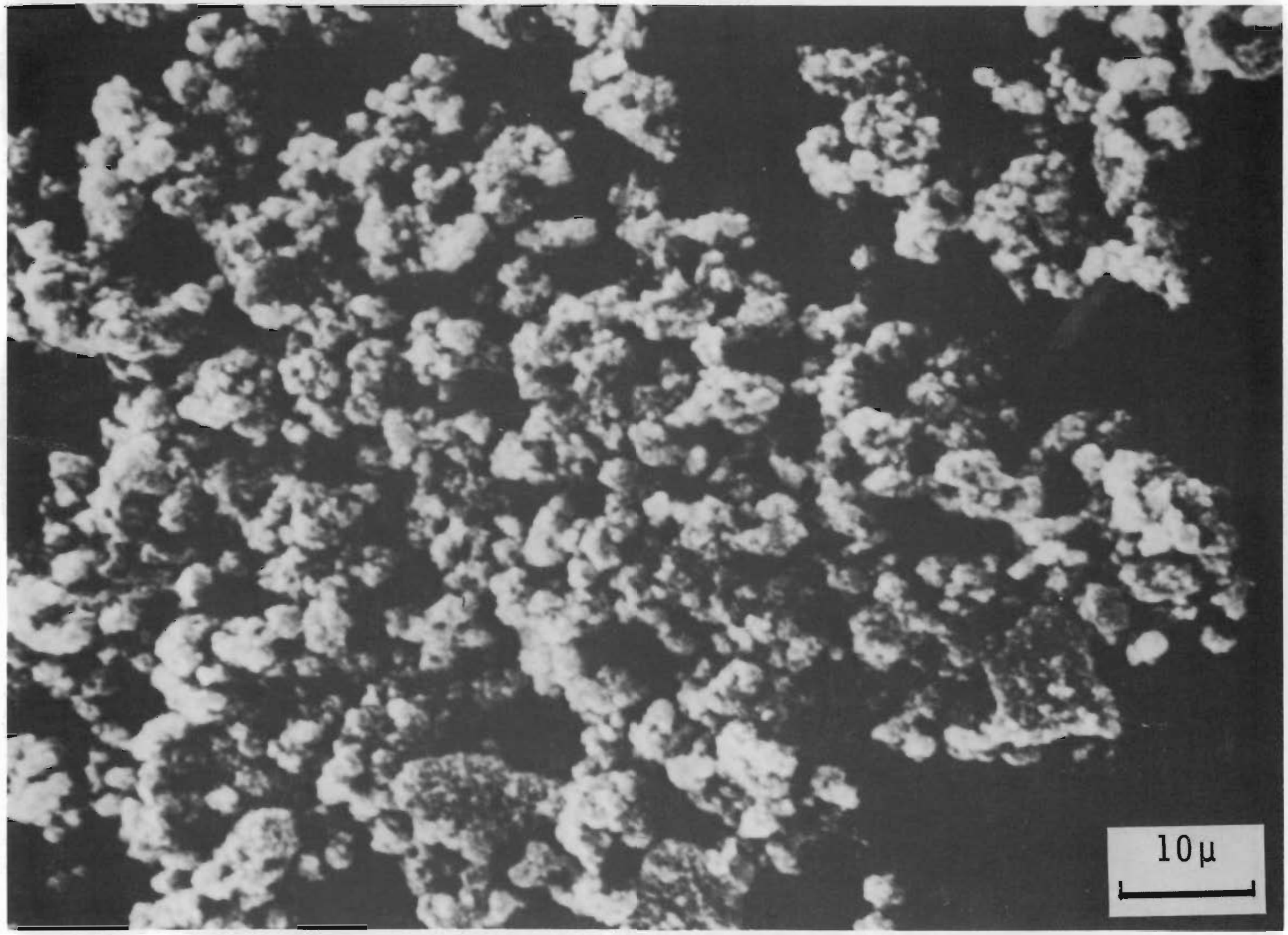

#659

FIGURE 3. SCANNING ELECTRON MICROGRAPH OF SOURCE A UO_2 - AS-RECEIVED

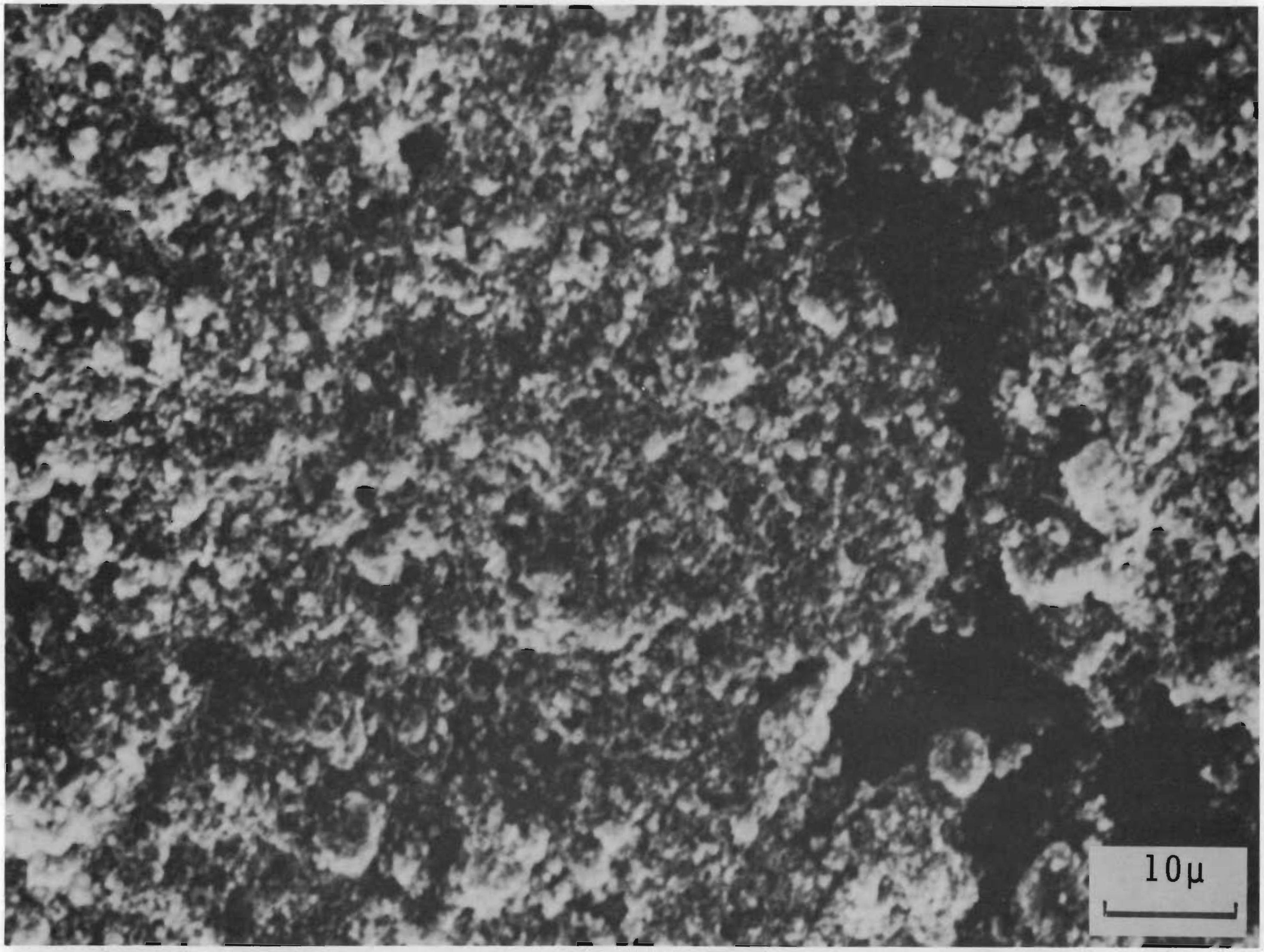

#622
FIGURE 4. SCANNING ELECTRON MICROGRAPH OF MILLED SOURCE A UO_2 (2000X)

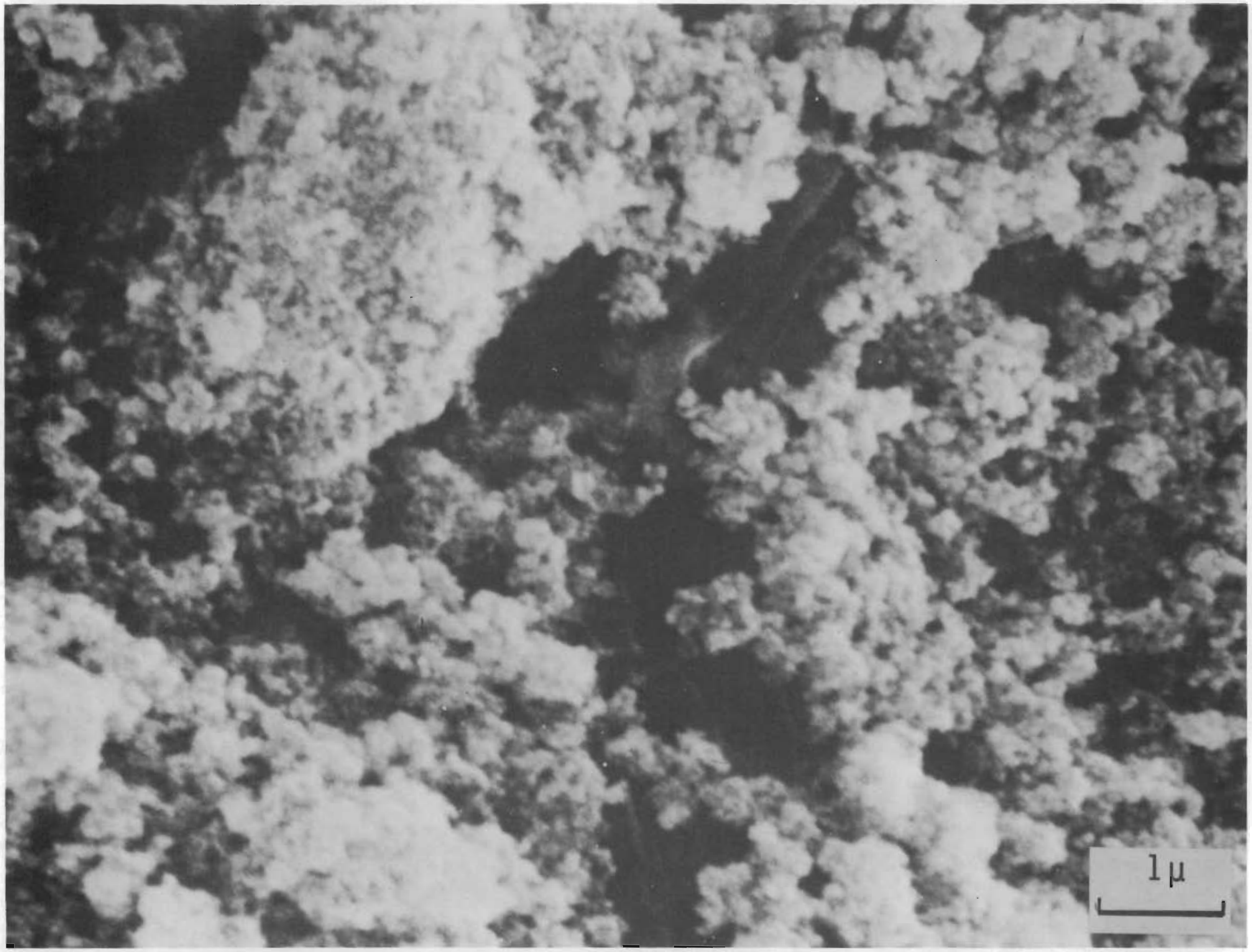

#684
FIGURE 5. SCANNING ELECTRON MICROGRAPH OF MILLED SOURCE A UO_2 (20,000X)

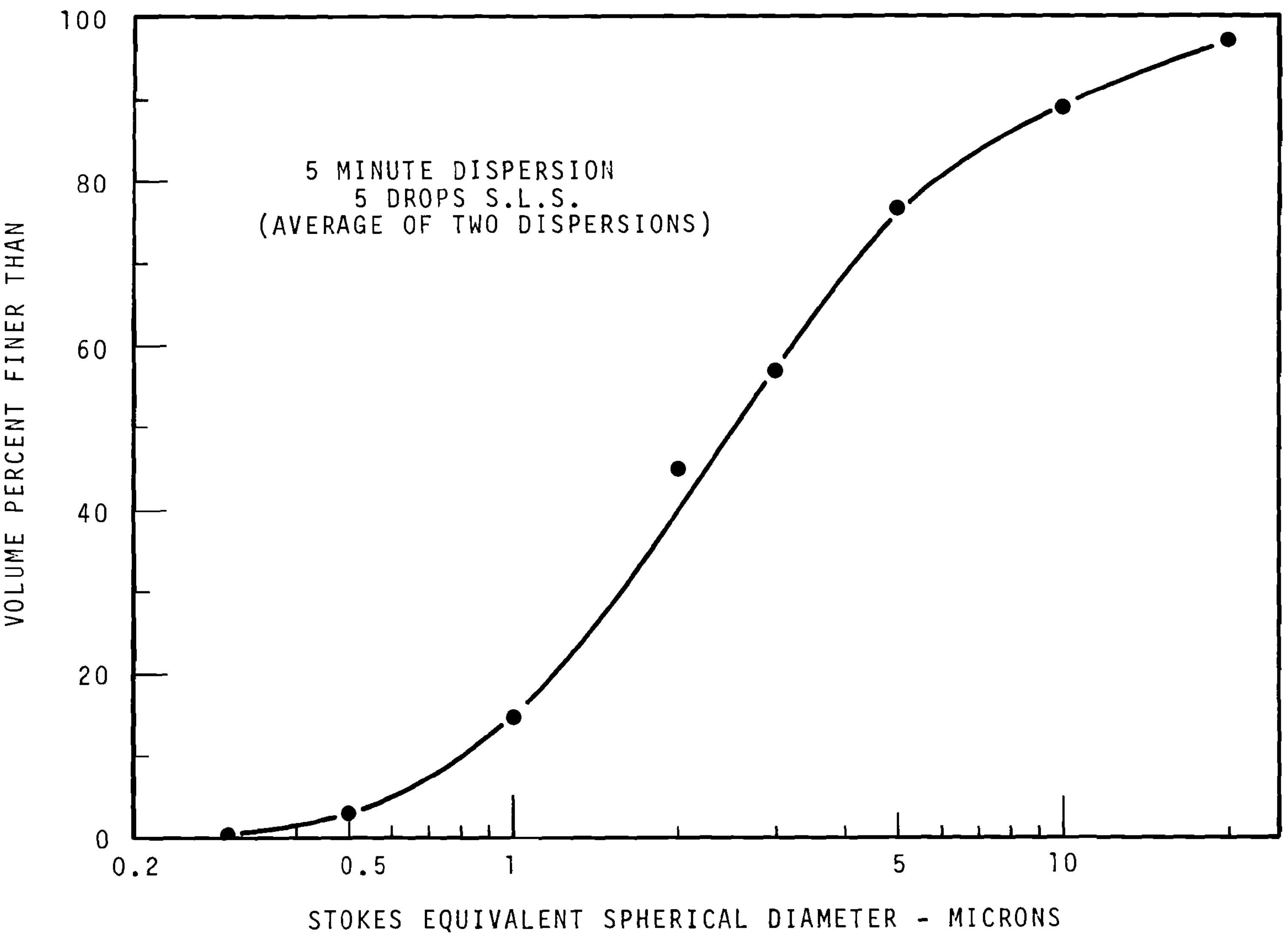

FIGURE 6. PARTICLE SIZE OF SOURCE B - AS-RECEIVED

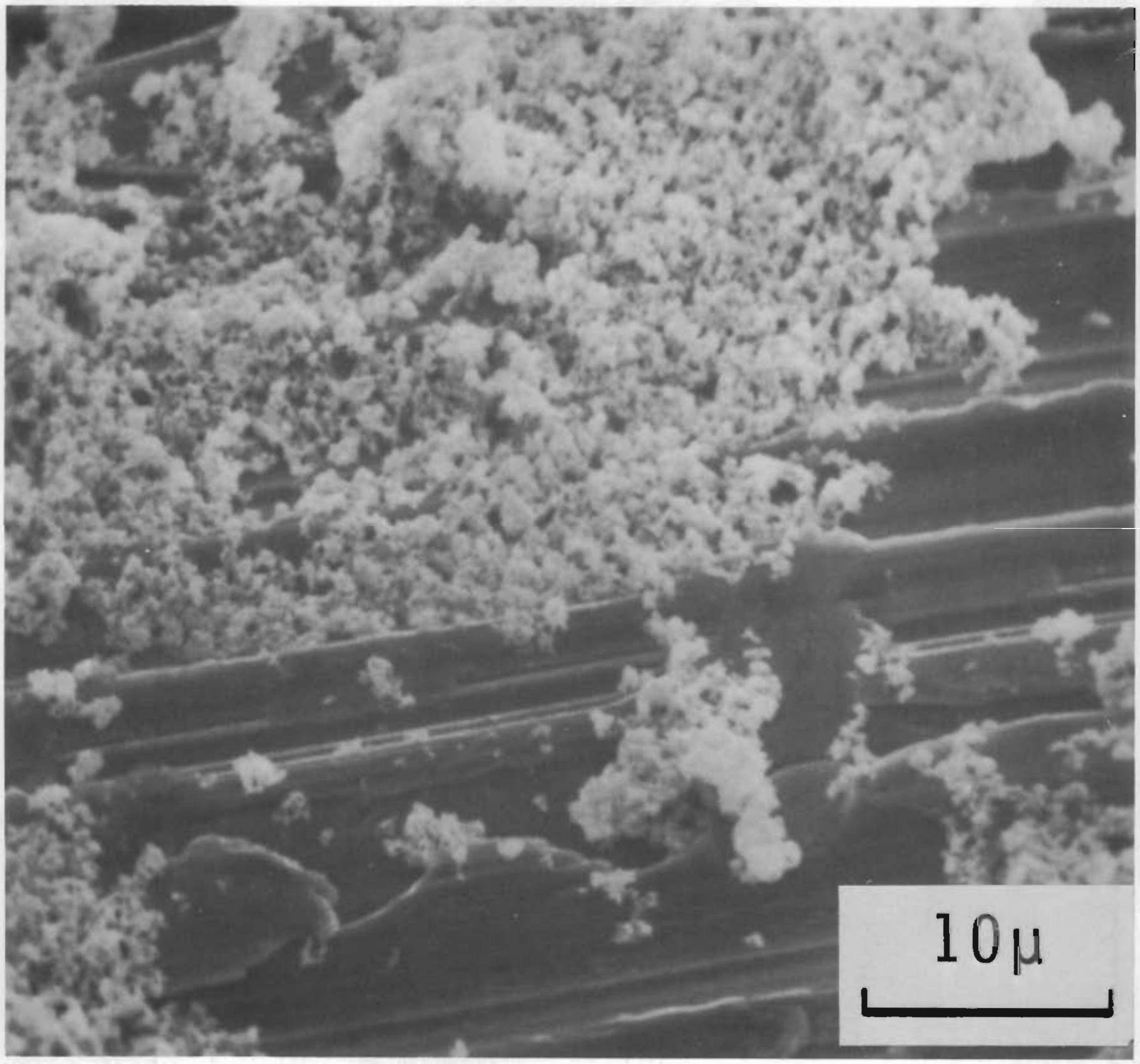

#3137

FIGURE 7. SCANNING ELECTRON MICROGRAPH OF SOURCE B UO_2 (3300X)

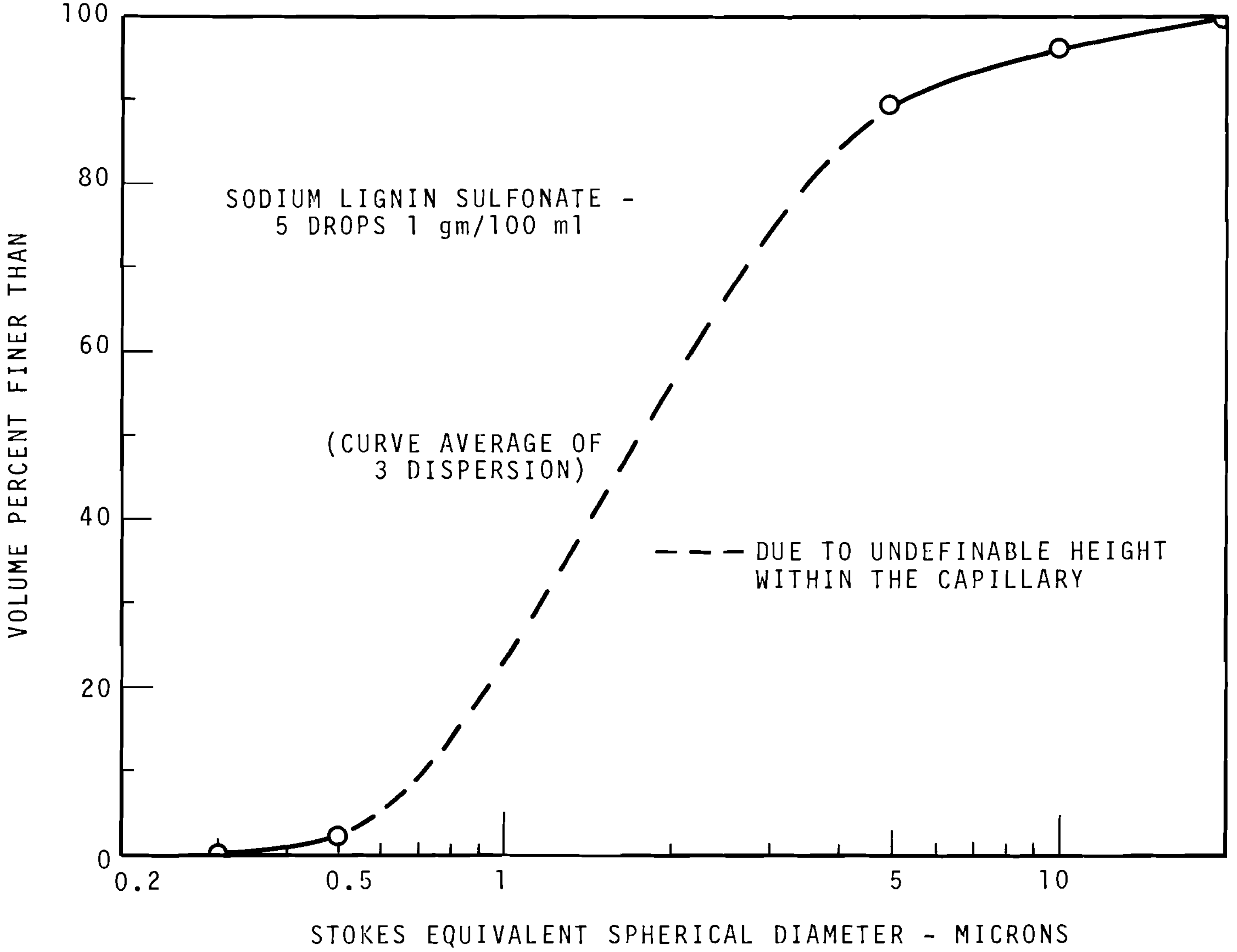

FIGURE 8. PARTICLE SIZE OF 93% ENRICHED UO_2

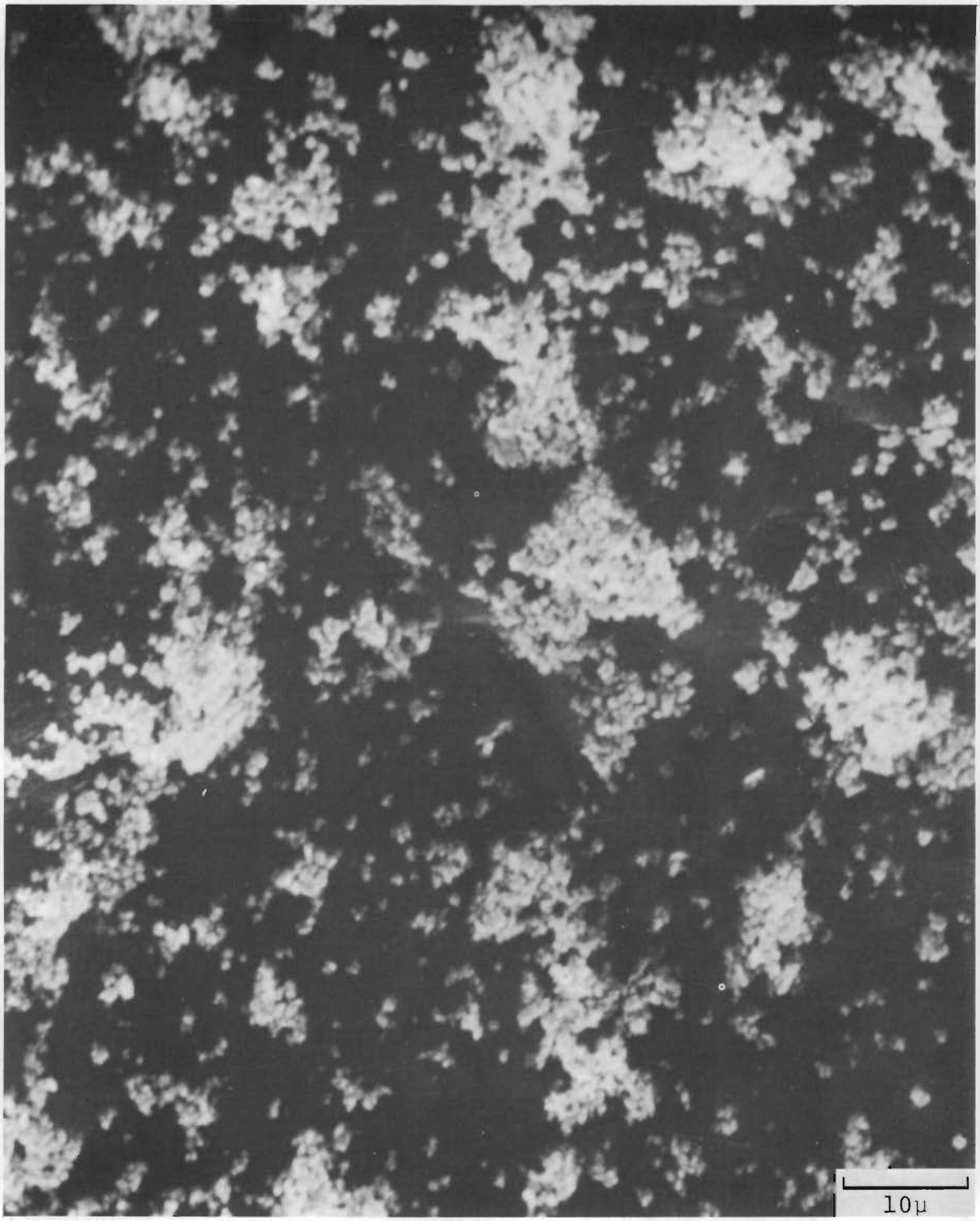

#681

FIGURE 9. SCANNING ELECTRON MICROGRAPH OF 93% ENRICHED UO_2 (2000X)

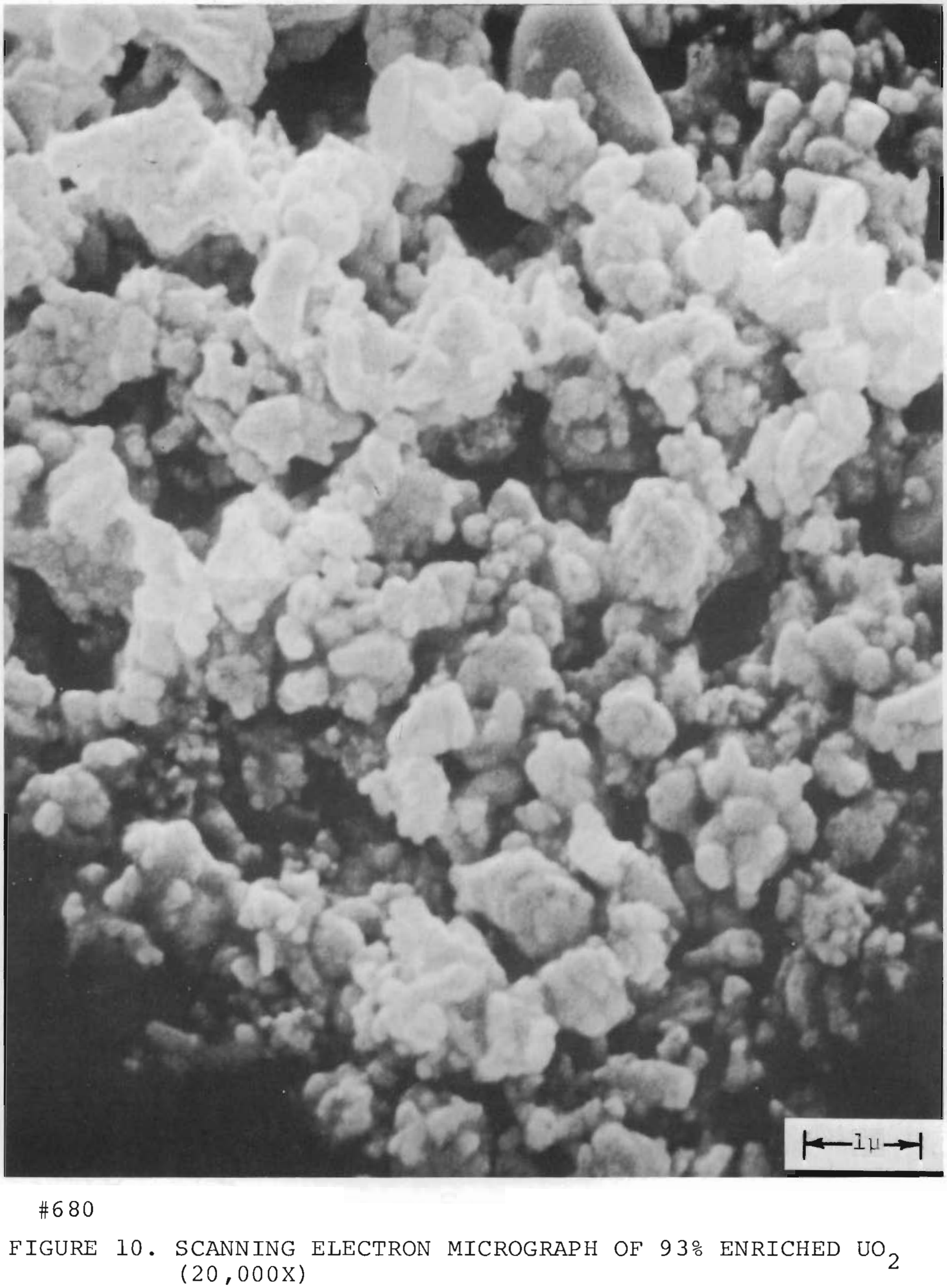

#680

FIGURE 10. SCANNING ELECTRON MICROGRAPH OF 93% ENRICHED UO_2 (20,000X)

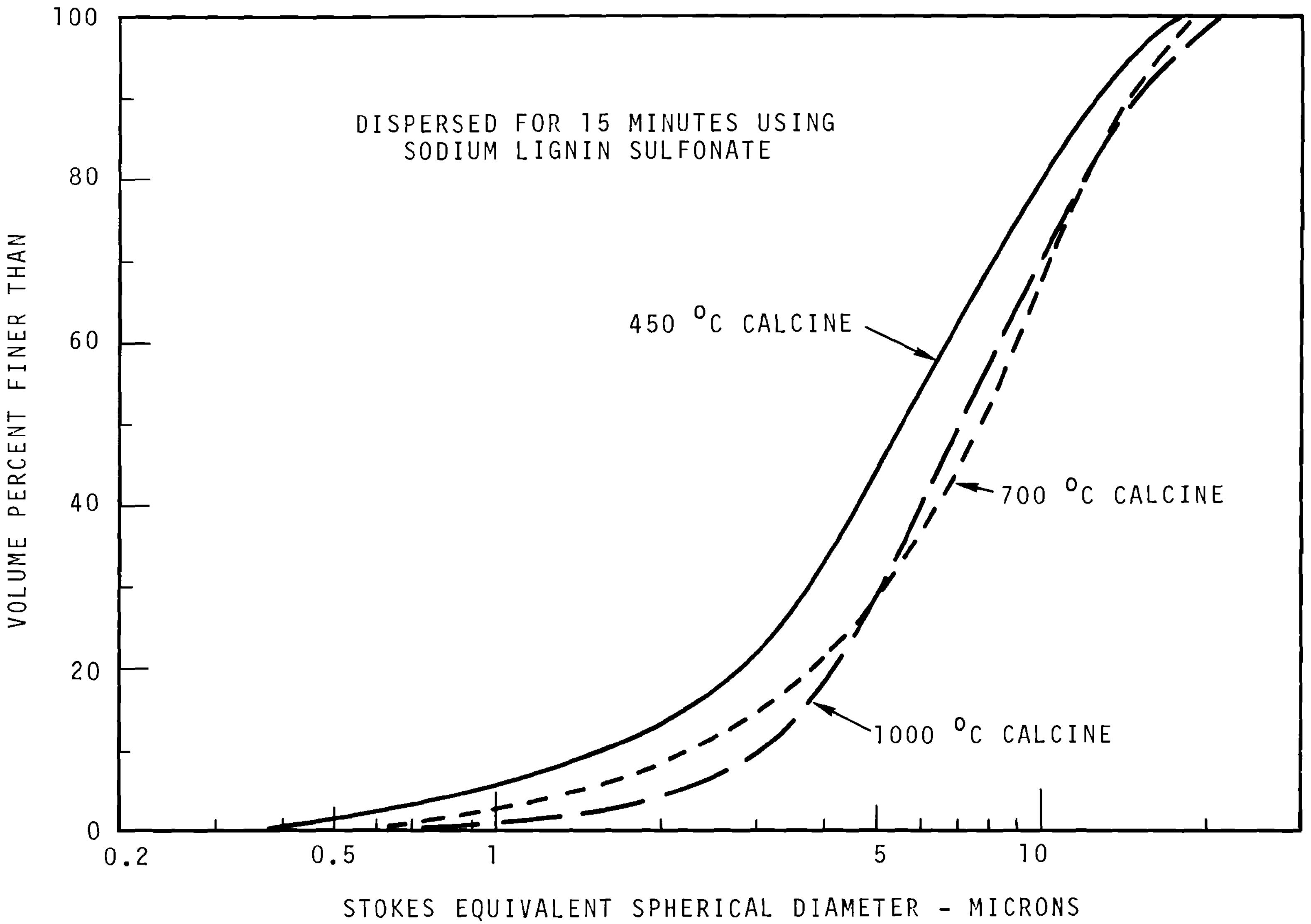

FIGURE 11. PARTICLE SIZE OF CALCINED OXALATE SOURCE PuO_2

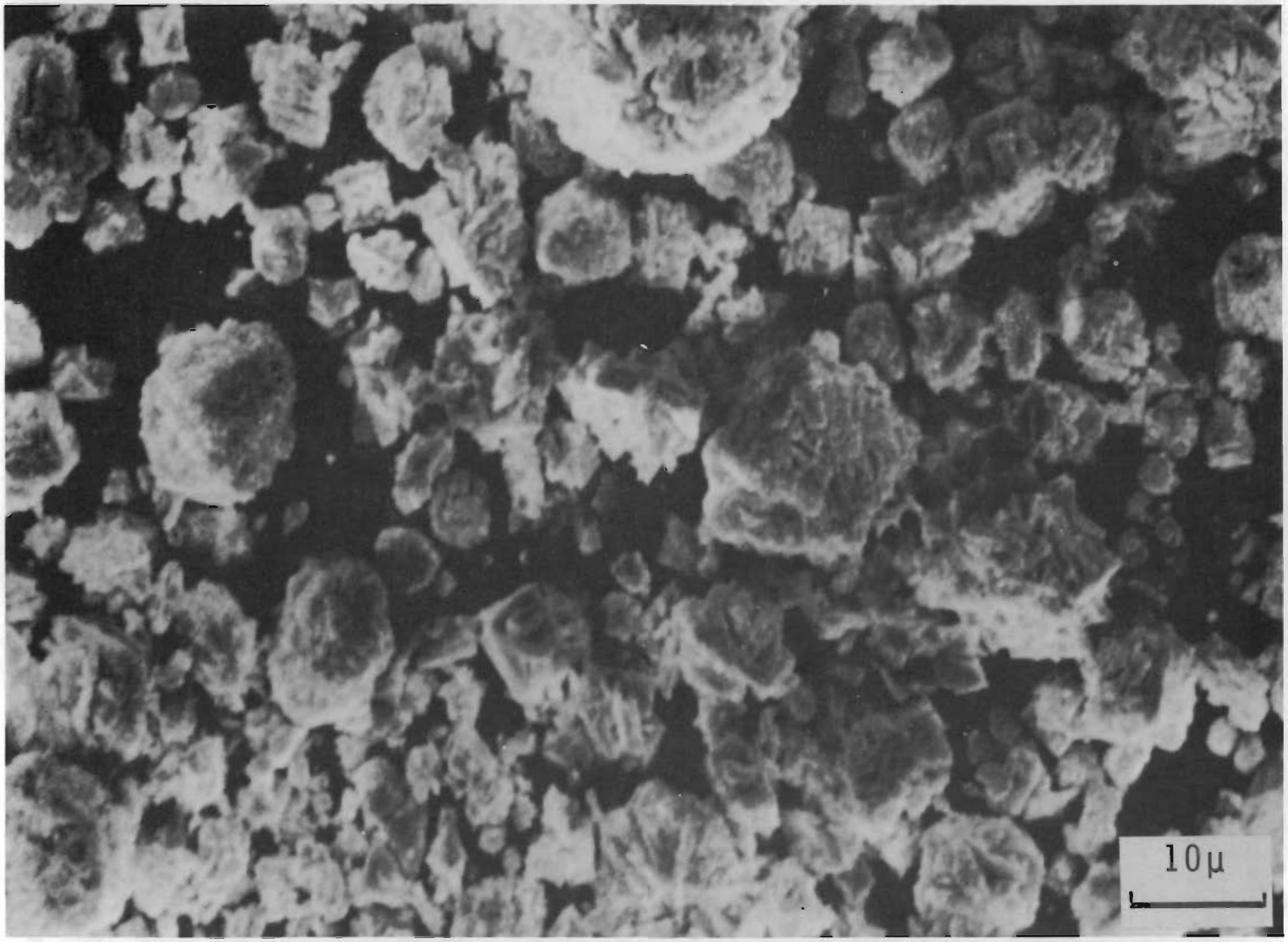

#1370

FIGURE 12. SCANNING ELECTRON MICROGRAPH OF 450 °C CALCINED OXALATE SOURCE PuO_2 (2000X)

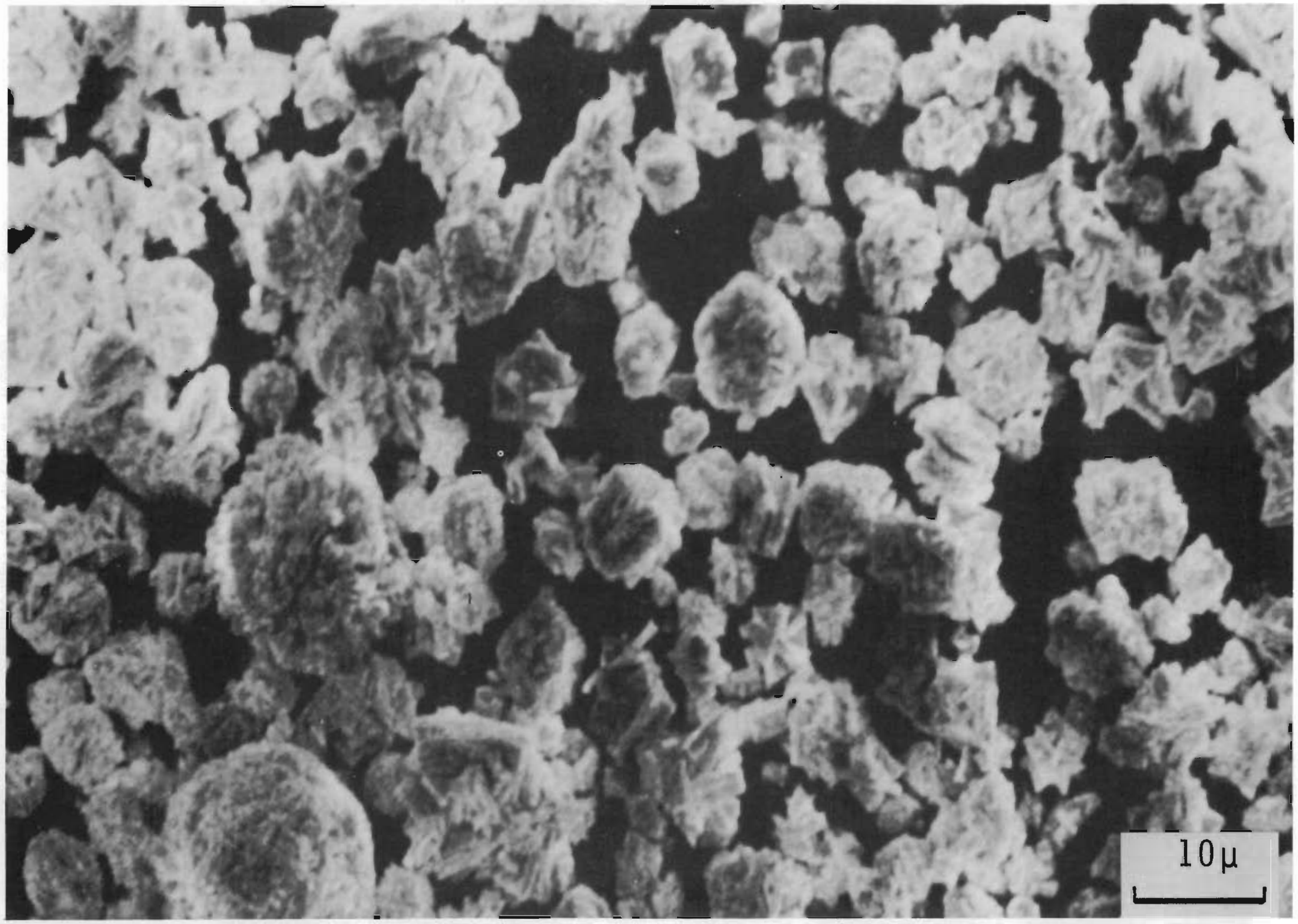

#1393

FIGURE 13. SCANNING ELECTRON MICROGRAPH OF 1000 °C CALCINED OXALATE SOURCE PuO_2 (2000X)

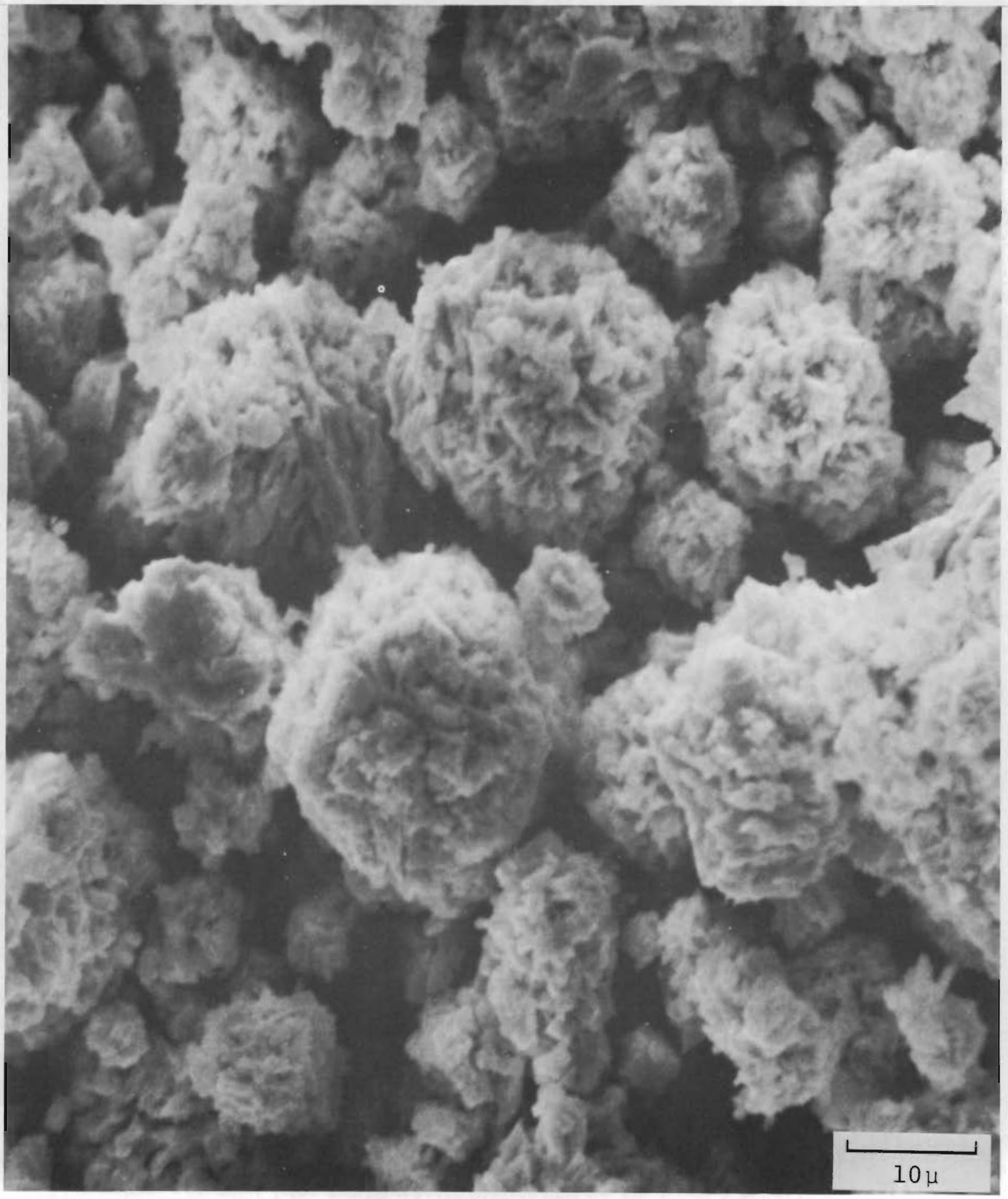

#1601

FIGURE 14. PLUTONIUM OXALATE [$Pu(C_2O_4)_2 \cdot 6H_2O$]

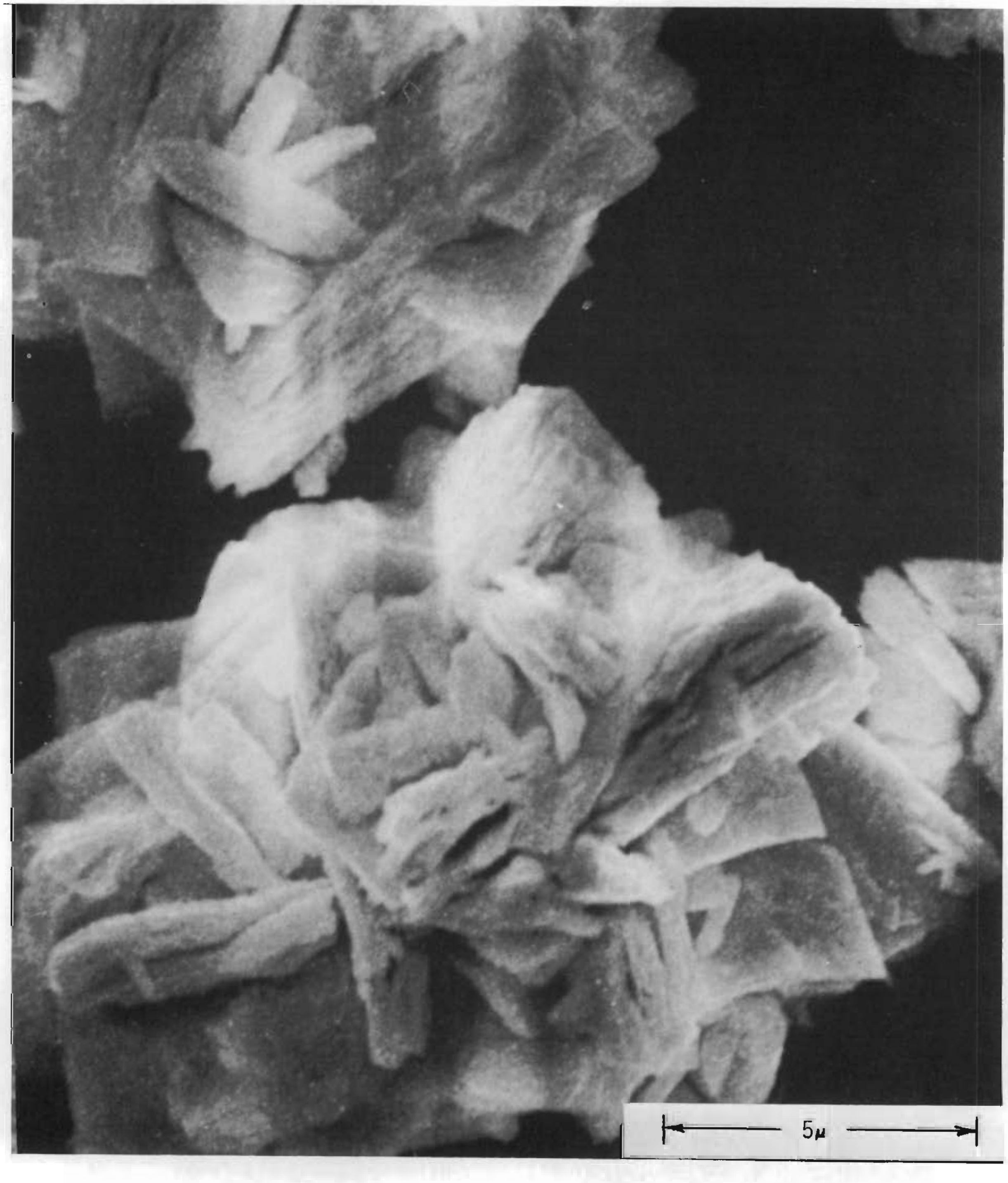

#1369

FIGURE 15. 450 °C CALCINED OXALATE SOURCE PuO_2 (10,000X)

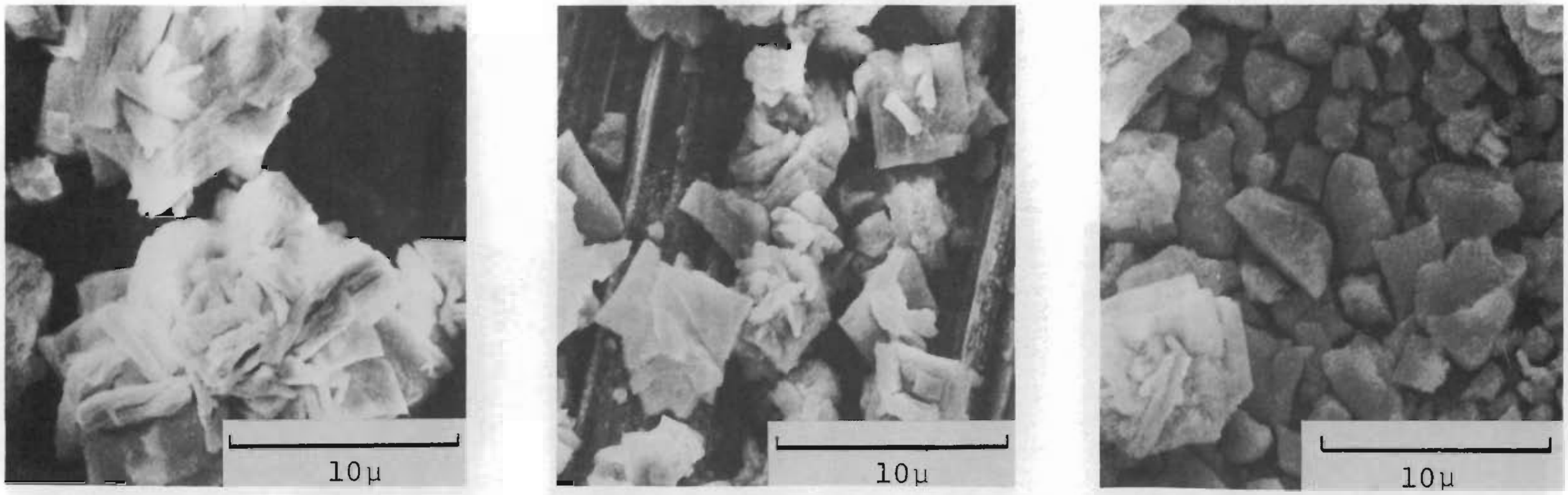

NO AGITATION
#1369

15 MINUTE AGITATION
#1641

120 MINUTE AGITATION
#1645

FIGURE 16. EFFECT OF ULTRASONIC AGITATION ON 450 °C CALCINED OXALATE SOURCE PuO_2

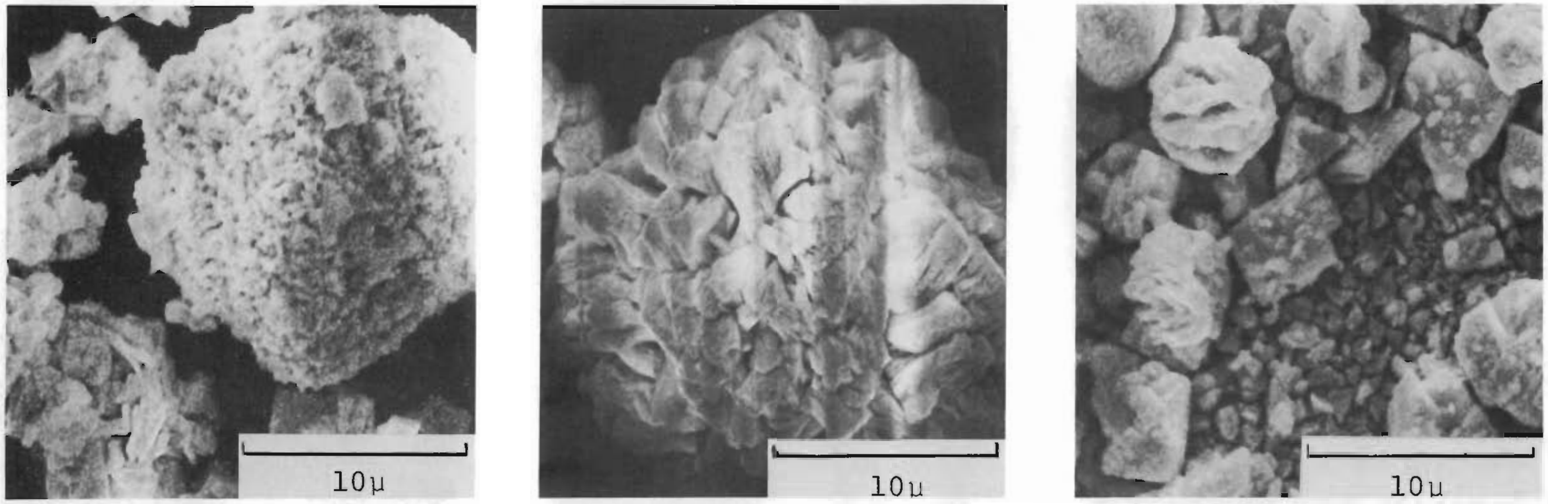

NO AGITATION
#1389

15 MINUTE AGITATION
#1633

120 MINUTE AGITATION
#1629

FIGURE 17. EFFECT OF ULTRASONIC AGITATION ON 1000 °C CALCINED OXALATE SOURCE PUO_2

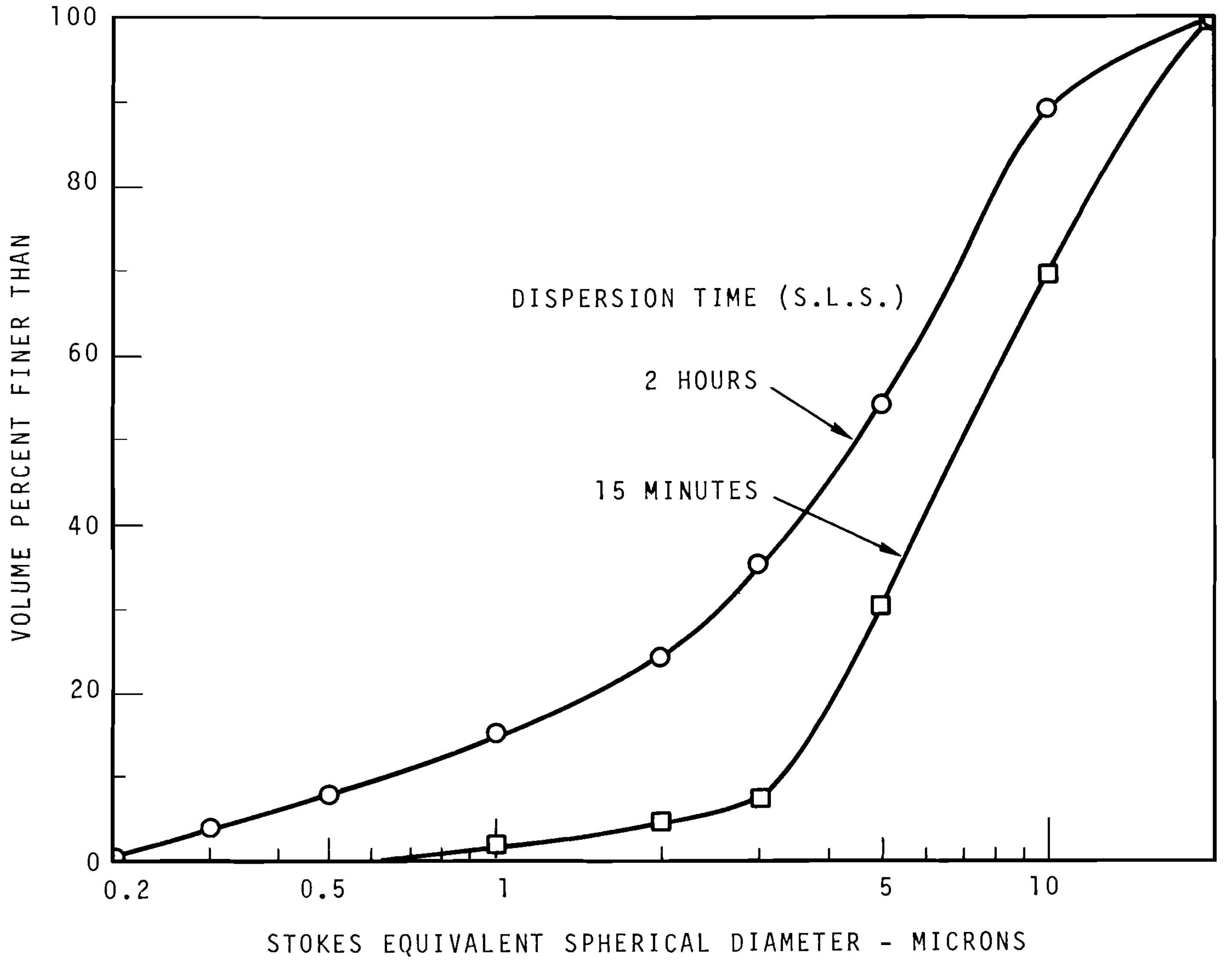

FIGURE 18. PARTICLE SIZE VERSUS DISPERSION TIME FOR 1000 °C CALCINED OXALATE SOURCE PuO_2

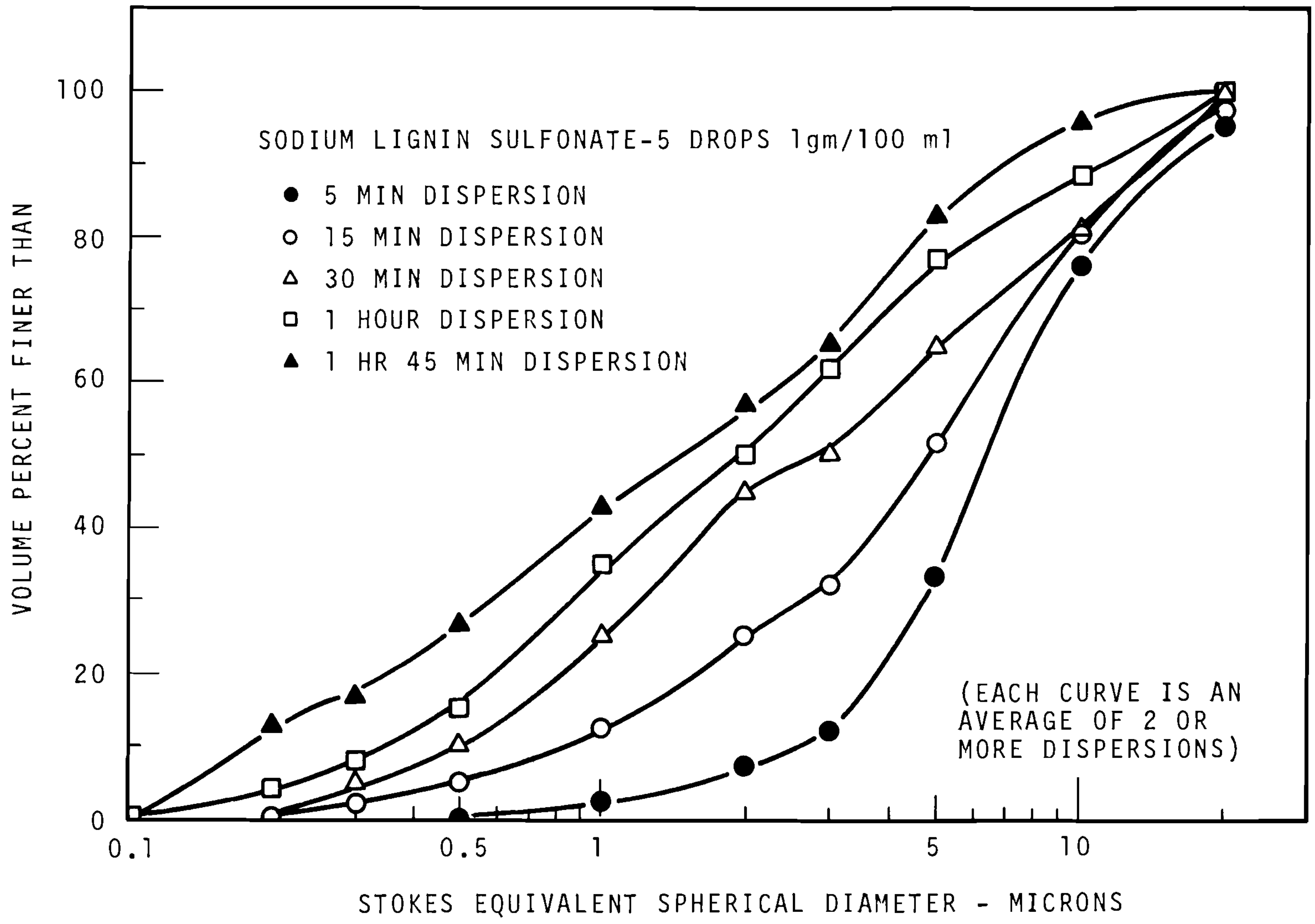

FIGURE 19. PARTICLE SIZE VERSUS DISPERSION TIME FOR 700 °C CALCINED OXALATE SOURCE PuO_2

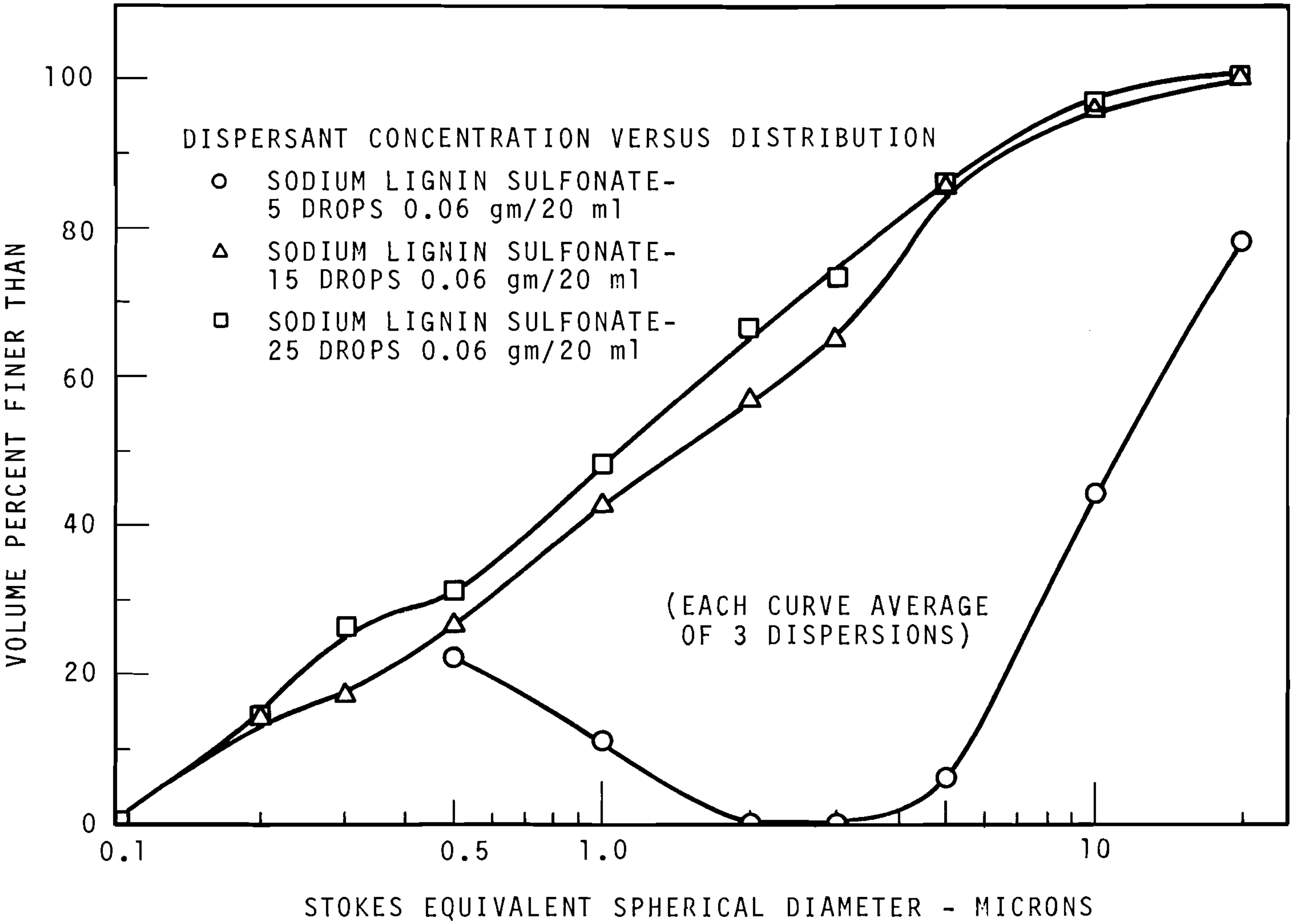

FIGURE 20. EFFECT OF DISPERSANT CONCENTRATION ON PARTICLE SIZE OF 450 °C CALCINED OXALATE SOURCE PuO_2 (2 HOUR DISPERSION)

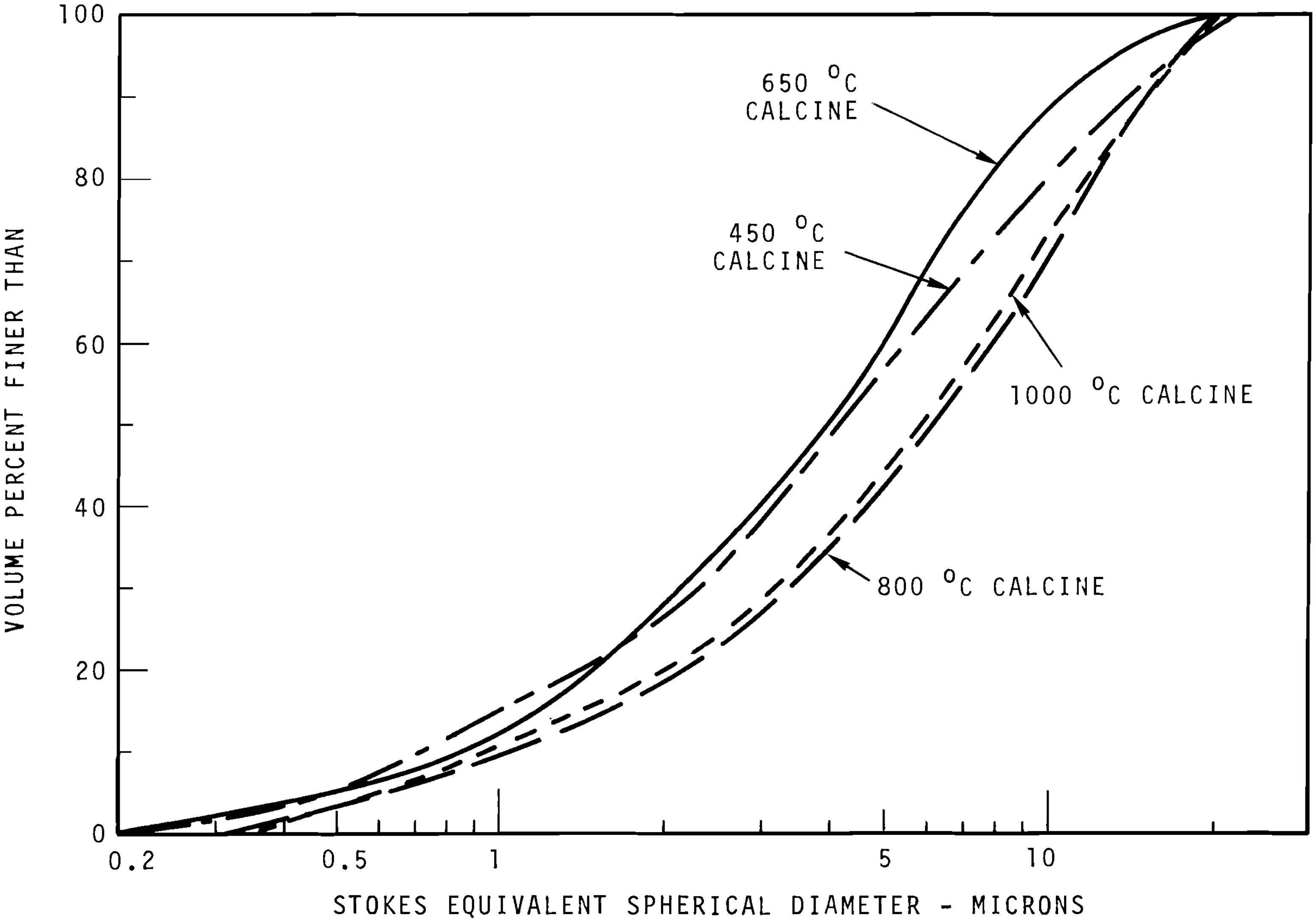

FIGURE 21. PARTICLE SIZE OF CALCINED NITRATE SOURCE PuO$_2$

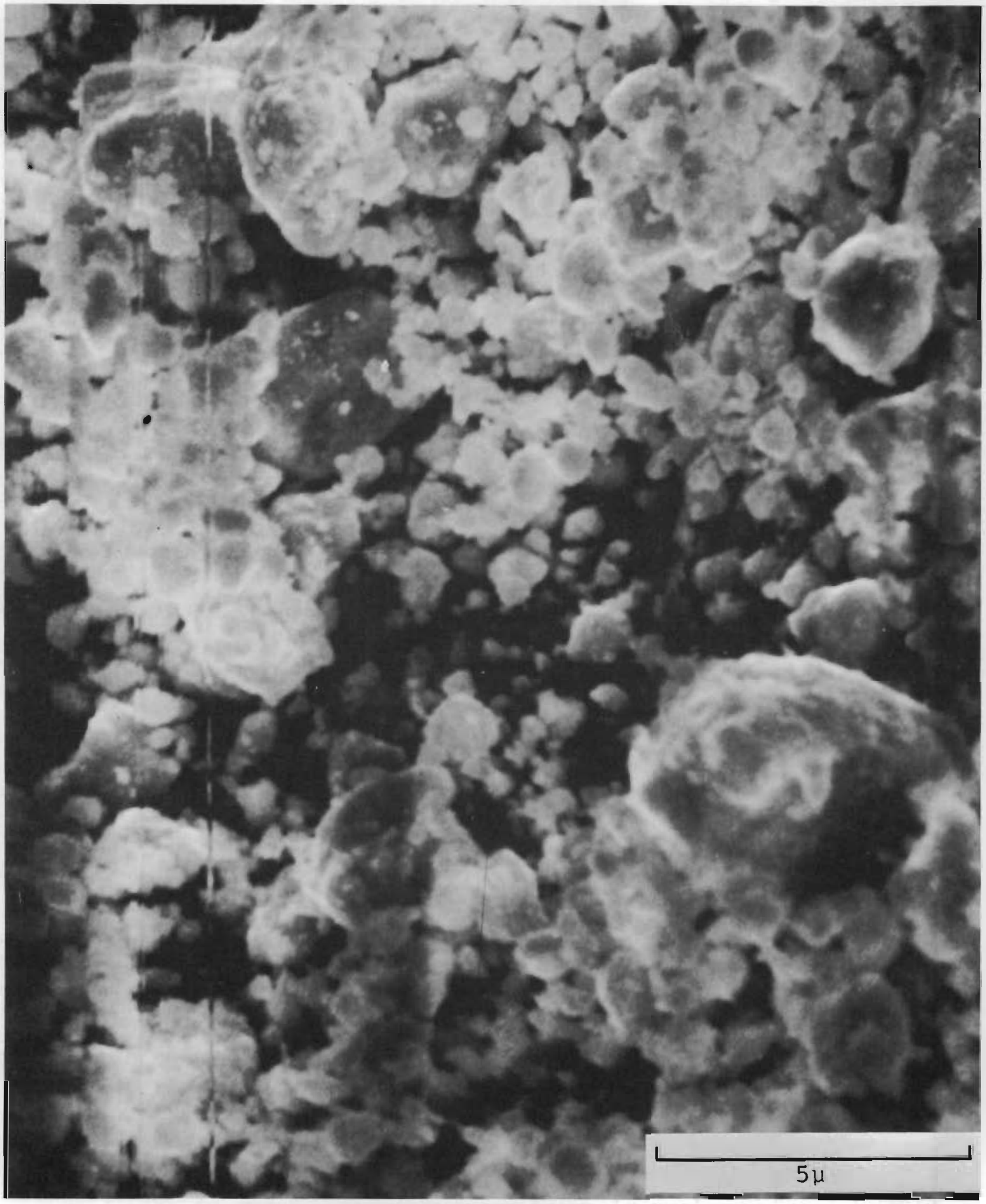

#1606

FIGURE 22. SCANNING ELECTRON MICROGRAPH OF 1000 °C CALCINED NITRATE SOURCE PuO_2 (10,000X)

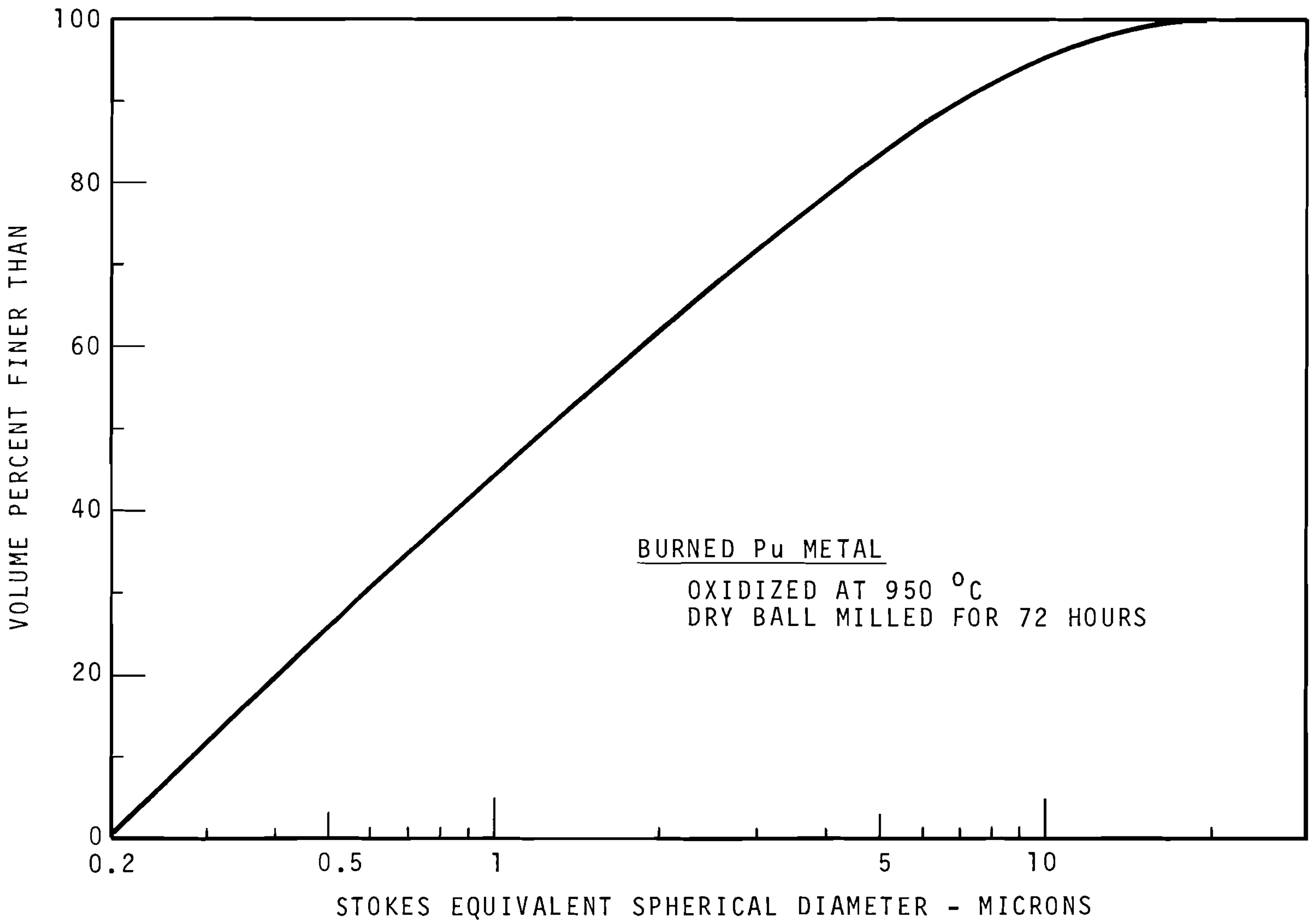

FIGURE 23. PARTICLE SIZE OF BURNED Pu METAL (PuO_2)

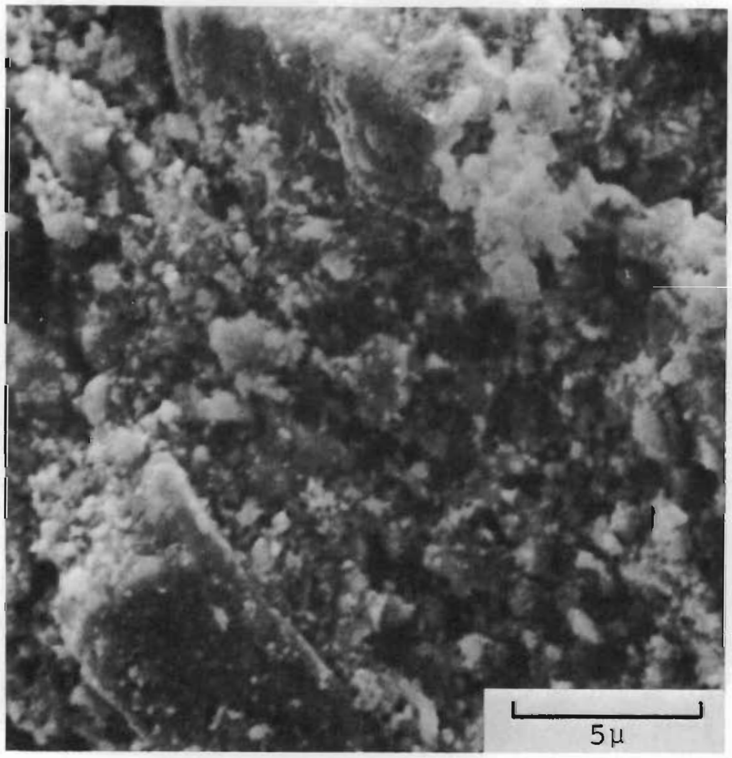

#3822

FIGURE 24. SCANNING MICROGRAPH OF BURNED Pu METAL (5000X)

DISTRIBUTION

No. of Copies	
OFFSITE	
1	AEC Chicago Patent Group G. H. Lee
210	AEC Division of Technical Information Extension
26	AEC Division of Reactor Development and Technology Director, RDT Asst Dir for Nuclear Safety Analysis & Evaluation Br, RDT:NS Asst Dir for Plant Engrg, RDT Facilities Br, RDT:PE Components Br, RDT:PE Instrumentation & Control Br, RDT:PE Liquid Metal Systems Br, RDT:PE Asst Dir for Program Analysis, RDT Asst Dir for Project Mgmt, RDT Liquid Metals Projects Br, RDT:PM G. J. Mishko FFTF Project Manager, RDT:RE Asst Dir for Reactor Engrg, RDT Control Mechanisms Br, RDT:RE Core Design Br, RDT:RE (2) Fuel Engineering Br, RDT:RE Fuel Handling Br, RDT:RE Reactor Vessels Br, RDT:RE Coolant Chemistry Br, RDT:RT Fuel Recycle Br, RDT:RT Fuels & Materials Br, RDT:RT Reactor Physics Br, RDT:RT Special Technology Br, RDT:RT Asst Dir for Engrg Standards, RDT LMFBR Program Manager, RDT:PM
1	AEC Idaho Operations Office Nuclear Technology Division C. W. Bills, Director
1	AEC San Francisco Operations Office Director, Reactor Division
5	AEC Site Representatives Argonne National Laboratory-CH Argonne National Laboratory-ID Atomics International General Electric Co. Westinghouse Electric Co.

No. of Copies	
3	Argonne National Laboratory R. A. Jaross LMFBR Program Office N. J. Swanson
1	Atomic Power Development Assoc. Document Librarian
5	Atomics International FFTF Program Office (5)
2	Babcock & Wilcox Co. Atomic Energy Division S. H. Esleeck G. B. Garton
10	Bechtel Corporation J. J. Teachnor, Project Administrator, FFTF
1	Combustion Engineering 1000 MW_e Follow-On Study W. P. Staker Project Manager
1	Combustion Engineering Mrs. Nell Holder, Librarian
4	General Electric Company Advanced Products Operation Karl Cohen
1	General Electric Company Nucleonics Laboratory Dr. H. W. Alter, Mgr.
2	Gulf General Atomic Inc. General Atomic Div. D. Coburn
1	Idaho Nuclear Corporation J. A. Buckham
1	Liquid Metal Information Center R. W. Dickinson
2	Liquid Metal Information Center A. E. Miller
1	Oak Ridge National Laboratory W. O. Harms

No. of Copies	
1	Stanford University Nuclear Division Division of Mechanical Engrg R. Sher
1	United Nuclear Corporation Research and Engineering Center R. F. DeAngelis
11	Westinghouse Electric Corporation Atomic Power Division Advanced Reactor D. C. Spencer
1	Westinghouse Electric Corporation (PFDL) Cheswick, Pennsylvania John Denero

ONSITE

1	AEC Chicago Patent Group R. K. Sharp (Richland)
3	AEC RDT Site REpresentative P. G. Holsted
4	AEC Richland Operations Office C. L. Robinson J. M. Shivley (3)
3	Battelle Memorial Institute
5	Battelle-Northwest Technical Information
1	Bechtel Corporation W. A. Smith (Richland)
3	Jersey Nuclear Company J. L. Jaech
1	Westinghouse Electric Corporation R. Strezelecki (Richland)

No. of
Copies

76 WADCO Corp.

G. J. Alkire
A. G. Anderson
H. J. Anderson
S. O. Arneson
J. M. Atwood
R. E. Bardsley
M. J. Barr (10)
J. M. Batch
H. T. Blair
C. A. Burgess
C. P. Cabell
J. R. Carrell
J. C. Cochran
G. S. Cochrane
D. L. Condotta
J. F. Erben
W. H. Esselman
E. A. Evans
W. M. Gajewski
K. M. Harmon
B. R. Hayward
E. N. Heck
P. L. Hofman
J. N. Judy
J. P. Keenan (5)
G. A. Last
F. J. Leitz
H. E. Little
W. B. McDonald
J. S. McMahon
J. M. Norris
R. E. Peterson
H. G. Powers
B. G. Rieck
W. E. Roake
G. J. Rogers
J. E. Sammis
W. F. Sheely
R. J. Squires
C. A. Strand
C. D. Swanson
J. W. Thornton
K. G. Toyoda
L. D. Turner
E. T. Weber
B. Wolfe
W. R. Wykoff
WADCO Document Control (15)
WADCO Tech Pubs (703)